Annales Geophysicae (2003) 21: 323–344

Annales Geophysicae

A high resolution hydrodynamic 3-D model simulation of the malta shelf area

A. F. Drago[1], **R. Sorgente**[2], **and A. Ribotti**[2]

[1]Physical Oceanography Unit, IOI-Malta Operational Cnt., University of Malta, c/o 36, Old Mint St., Valletta, VLT 12, Malta
[2]CNR-IAMC, Sect. Oristano, c/o International Marine Centre, Loc. Sa Mardini, 09072 Torregrande-Oristano, Italy

Received: 23 August 2001 – Revised: 6 May 2002 – Accepted: 17 June 2002

Abstract. The seasonal variability of the water masses and transport in the Malta Channel and proximity of the Maltese Islands have been simulated by a high resolution (1.6 km horizontal grid on average, 15 vertical sigma layers) eddy resolving primitive equation shelf model (ROSARIO-I). The numerical simulation was run with climatological forcing and includes thermohaline dynamics with a turbulence scheme for the vertical mixing coefficients on the basis of the Princeton Ocean Model (POM). The model has been coupled by one-way nesting along three lateral boundaries (east, south and west) to an intermediate coarser resolution model (5 km) implemented over the Sicilian Channel area. The fields at the open boundaries and the atmospheric forcing at the air-sea interface were applied on a repeating "perpetual" year climatological cycle.

The ability of the model to reproduce a realistic circulation of the Sicilian-Maltese shelf area has been demonstrated. The skill of the nesting procedure was tested by model-model comparisons showing that the major features of the coarse model flow field can be reproduced by the fine model with additional eddy space scale components. The numerical results included upwelling, mainly in summer and early autumn, along the southern coasts of Sicily and Malta; a strong eastward shelf surface flowalong shore to Sicily, forming part of the Atlantic Ionian Stream, with a presence throughout the year and with significant seasonal modulation, and a westward winter intensified flow of LIW centered at a depth of around 280 m under the shelf break to the south of Malta. The seasonal variability in the thermohaline structure of the domain and the associated large-scale flow structures can be related to the current knowledge on the observed hydrography of the area. The level of mesoscale resolution achieved by the model allowed the spatial and temporal evolution of the changing flow patterns, triggered by internal dynamics, to be followed in detail.

This modelling effort has initiated the treatment of the open boundary conditions problem in view of the future implementation of shelf-scale real-time ocean forecasting through the sequential nesting of a hierarchy of successively embedded model domains for the downscaling of the hydrodynamics from the coarse grid Ocean General Circulation Model of the whole Mediterranean Sea to finer grids in coastal areas.

Key words. Oceanography: general (continental shelf processes; numerical modelling) Oceanography: physical (general circulation)

Correspondence to: A. F. Drago (aldo.drago@um.edu.mt)

1 Introduction

Around 20% of all oil transported by sea traverses the Mediterranean, amounting to an annual flux of 350 million tons of crude oil and refined products. Most of this maritime traffic travels across the Malta Channel or passes in propinquity to the southern approaches of the Maltese Islands. Besides oil, many other liquid substances are conveyed in large quantities by sea-routes traversing this region. With the development of the ports in Malta, in particluar, with the proliferating activity at the freeport, and the enhanced reputation of the island for the provision of a comprehensive range of maritime services, the volume of seafaring vessels visiting this part of the Mediterranean continues to increase. This renders the Malta Channel and the Maltese shelf area one of the highest risk zones to marine pollution from oil and other hazardous substances. An adequate response to such risks requires a sufficient base of oceanographic information in support of risk-prediction models and decision systems for prevention measures or in case of emergency interventions.

From the fisheries' point of view, the fish populations over the Malta platform area are considered to be an independent management unit stock, especially for shelf demersal resources (Camilleri, 2000). Except for rather narrow pathways, the continental shelf of Malta is disconnected from the adjacent shallow sea areas and ground-fish species are believed to be somewhat isolated. The limited extent of this

area accentuates the vulnerability of the ecosystem and calls for precautionary measures against unsustainable fishing efforts and bad fishing practices.

Notwithstanding this need, the region remains one of the least studied in the Mediterranean to date. Within the MEDATLAS-I (1997) data set there are just 104 CTD stations, together with 1014 XBT and 1407 MBT profiles in the 2-degree square centered on 14° E and 36° N. Sea current measurements are, however, generally lacking. The most comprehensive sea current data refers to the section between Sicily and Libya, which was studied by AGIP in the framework of the Libyan Offshore to Sicily Gas Transportation System Project, and conducted during July 1981 – July 1982 (Grancini, 1985) by the Osservatorio Geofisico Sperimentale of Trieste. The array of moorings included a station on the Sicilian shelf to the east of Malta. More recently, currents in the northwestern coastal area of Malta were conducted in the period 1993–1994 (Drago, 1995). On the other hand, coverage by satellite-derived thermal infra-red images (Le Vourch et al., 1992; Champagne-Philippe and Harang, 1982) and ocean colour data in this relatively cloud-free region has offered the means to identify the synoptic variability and the mesoscale phenomena in this dynamically active area. In particular, this has enabled a detailed characterization of one of the most important Mediterranean upwelling systems along the southern coast of Sicily (Kostianoy et al., 1998). Nonetheless, the three-dimensional thermohaline structure, as well as the dynamics and seasonal variability in the Malta shelf area, is not sufficiently studied.

We can resort to numerical modelling as an additional useful tool to improve the knowledge on the phenomenology and variability of ocean processes pertaining to the area. Previous modelling studies have, however, incorporated this part of the Mediterranean within a coarser and larger (basin) scale context. This work is a first dedicated model application in the area of interest, attempting to describe the seasonal variability of the hydrodynamics by a climatological simulation, using a mesoscale-admitting implementation of a nested version of the Princeton Ocean Model (POM). It forms part of the general shelf modelling effort conducted during the first phase of the Mediterranean Forecasting System Pilot Project (MFSPP) (Pinardi, 1998; Pinardi et al., 1999, 2003) in which one-way off-line interactions between a series of successively embedded model domains have been shown to efficiently downscale model solutions from the basin-scale ($\approx$12.5 km) to the regional-scale (4–5 km) and to the high resolution shelf-scale (1.5–2 km) implementations.

Indeed, computational constraints pose the need to embed high resolution fine grid models into larger coarser resolution domains. This necessitates the use of adequate nesting techniques to enable an efficient inter-grid flow of information. The nested-grid technique has been widely used in meteorological models (Koch and McQueen, 1987). The first attempts to apply the method to the ocean, such as by Oey (1986), Galerpin and Mellor (1990) and Spall and Holland (1991), have been followed in the past decade by several other applications (e.g. Oey and Chen, 1992; Fox and Maskell, 1996; Oey, 1998), showing that nesting boundary conditions have to be somewhat customised to suit different model implementations, specific flow conditions and open boundaries (Pinardi et al., 2002). In the context of limited area high numerical resolution models, the nesting specification is even more stringent, since the changes occurring at the lateral boundaries have the same space and time scales as the internal flow field, and the fine model solution is very strictly influenced by the flow conditions remote to the model domain.

The main goal of this study is to demonstrate the feasibility of free-surface/free-surface models nesting on a climatological basis, using complex primitive equation models with active thermodynamics, implemented over a shelf-scale inner domain (high resolution) covering the Malta Channel and Maltese shelf area (ROSARIO-I), and a regional-scale outer domain (coarse resolution) solution covering the Sicilian Channel area. The geographic configuration of the area, together with the need for a sufficiently fine grid and consequently, a limited domain extent, forces the inner model to have three open lateral boundaries to the west, south and east (Fig. 2). In this application, the MFSPP one-way nesting methodology has been adopted and tested in the case of three lateral boundaries. The choice of open boundary conditions was assessed for computational efficiency and the ability to minimize distortions at the nested grid boundaries, while allowing the large scales generated on the outer model to influence effectively the nested grid. The shelf model has been validated against the realistic representation of the known phenomenology and seasonal signatures in the climatological shelf circulation pertaining to this area. Furthermore, the model results have been used to furnish some deeper insights on the current knowledge from hydrographic observations and on the shelf dynamics pertaining to the area.

In the present work, the performance of the nesting technique is assessed, and the results of the shelf model climatological run are presented. The oceanography of the region is briefly reviewed in Sect. 2. The model setup is described in Sect. 3, with a focus on the nesting details. The model results are then described in Sect. 4, where the major dynamical features and variability of the climatological circulation are presented, together with the skill of the model, to elucidate the mesoscale activity in the area, especially that associated with internal dynamics. Section 5 presents a discussion and summary of the model results.

2 Bathymetry, meteorology and physical oceanography of the region

The region under consideration is the southeastern continental shelf of Sicily, presenting a rather complex bathymetry in the form of a large, roughly square bank with the Maltese Islands, residing on its southernmost extremity (Fig. 1). The shelf is interrupted from its extension towards the west by the relatively deep Gela Sicilian basin, separating it from the Adventure Bank. On its eastern extremity, it deepens

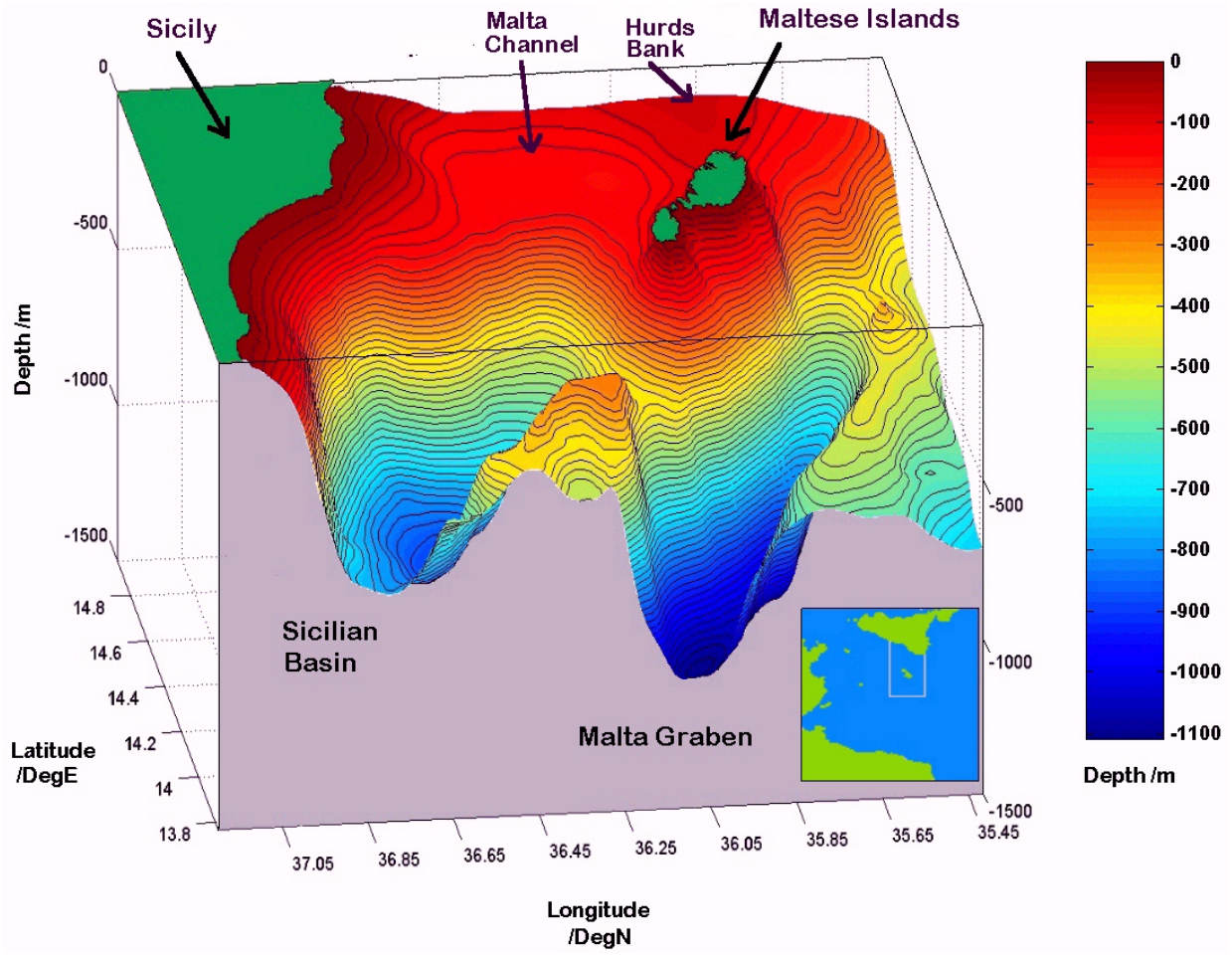

Fig. 1. Three-dimensional view of the model bathymetry (based on the U.S. Navy DBDB1 data set).

abruptly into the deep Ionian Sea, with a very sharp escarpment (known as the Malta Escarpment). The Malta Graben to the southwest of Malta forms part of a cluster of flat-bottomed depressions reaching a depth of around 1650 m. In its shallower parts, the shelf is characterized by a plateau in the middle part, with an average depth of 150 m. The shelf is flanked by a submarine ridge protruding in the form of a submerged extension of Cape Passero and embracing the shelf area along the eastern and southern perimeter. The Maltese Islands represent the emerged part of this ridge, while the Hurds Bank to the northeast of Malta shallows to a depth of just over 50 m. The islands are very close to the shelf break and flanked by a very steep bathymetry in the south.

As in the rest of the Mediterranean, atmospheric forcing plays a major role in the evolution of the upper ocean phenomenology (Pinardi et al., 1997). Knowledge of the prevailing meteo conditions is thus essential. Light to moderate winds prevail in this region for most of the time, but strong winds can be experienced almost throughout the year, although their frequency is much less during summer when pressure gradients are usually less. The percentage frequency of calm is only 13%. The prevailing wind, especially during the winter months, is the northwesterly (Mistral) wind which blows on average about 103 days a year, usually in periods of three days. It is often associated with lows that develop over northern Italy and move towards the east, down the Adriatic. The Mistral is favourable to coastal upwelling along the southern perimeter of Sicily. During summer, the northerly and northeasterly winds become equally dominant to wind blowing from the northwest. The northeast (Gregale) wind is not frequent but generally rises to gale force during the period between December to February, while strong southeasterly (Scirocco) winds of continental tropical origin usually occur towards late winter or in the April/May transition.

The hydrodynamics in the area is mainly dictated by the general flow in the Sicily Channel. The slow Mediterranean thermohaline basin scale circulation maintains a two-layer flow consisting of a fresh Modified Atlantic Water (MAW) eastward surface flow, and a deeper saltier westward Levantine water flow. The energetic and meandering Atlantic Ionian Stream (AIS) (Robinson et al., 1996) characterizes the surface circulation throughout the year. This swift topographically controlled current starts its path as a meander to the south of Adventure Bank. It then proceeds southeast-

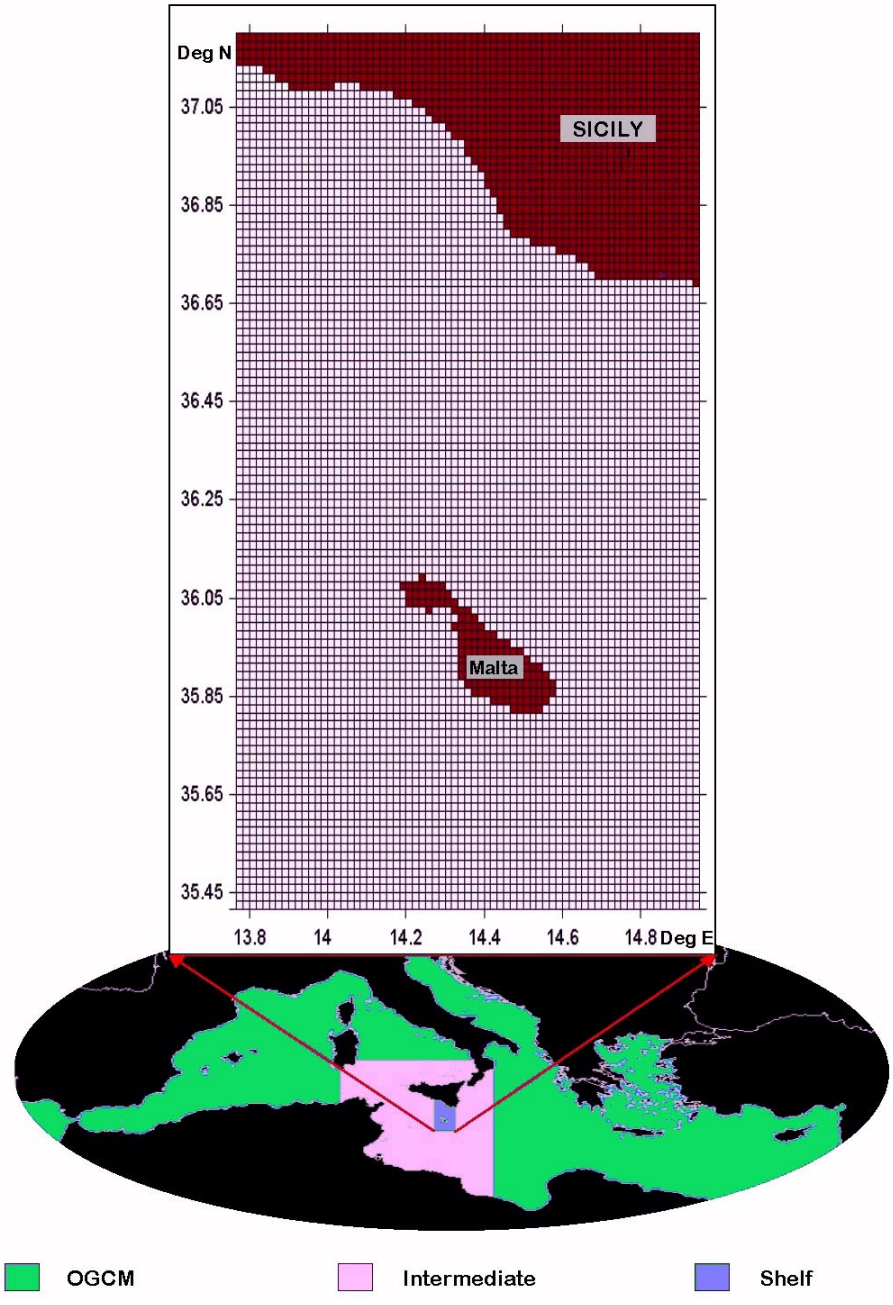

Fig. 2. The model gridded domain and its nesting to the intermediate model and the Ocean General Circulation Model of the Mediterranean.

wards and loops back northward around Malta, forming the Maltese Channel Crest. As it reaches the sharp shelf break to the east of Malta, it abruptly gains positive vorticity and tends to deflect with an intense looping northward meander, forming the characteristic Ionian Shelf Break Vortex. The progression of the AIS towards the east carries with it the fresh Modified Atlantic Water (MAW) across the Malta Channel. The contrast in temperature of the exiting MAW with the warmer Ionian Sea produces the Maltese Front which constitutes a conspicuous thermal filament on sea surface temperature AVHRR maps. The heat and momentum fluxes at the air-sea interface greatly contribute to the mixing and preconditioning of the MAW on its way to the Ionian Sea. Frequent coastal upwelling events bring to the surface cool water that is then swept along by the mesoscale eddy formations. The upwelling zone runs along the whole southern coast of Sicily and generally extends for a considerable distance (∼100 km) offshore, especially over Adventure Bank and on the Malta platform. The southeastward advection of these cold patches, in the form of long plumes and filaments, are a very characteristic feature in the thermal IR images of the region. Thus, the Sicilian upwelling produces a large influence on the upper layer dynamics in the region and has important implications on the biological productivity and the activity of the fisheries. During the colder months, surface cooling, due to the influence of polar air masses, can

result in the formation of large patches of relatively cooler water which accentuate the latitudinal thermal gradients in the northern parts of the strait, and enhance the contrast with the relatively warmer Ionian water at the Maltese Front.

The body of knowledge on the hydrodynamics pertaining to the area is used as a benchmark to assess the skill of the high resolution model implemented in the Malta Channel and Maltese shelf area. This numerical simulation is the first kind of its nature in this part of the Mediterranean. The results are useful to build a more comprehensive picture of the phenomenology and variability of the circulation in the region. It moreover presents an interesting case of flow around an island system, with an asymmetrical surrounding bathymetry and in proximity to a swift stream.

3 Model description and setup

The numerical code used is based on an application of the Princeton Ocean Model, POM (Blumberg and Mellor, 1987). POM is a primitive equation, stratified and nonlinear numerical ocean model which utilises the Boussinesq approximation and hydrostatic equilibrium. It uses the free surface, potential temperature and salinity, the three orthogonal components of velocity, the turbulence kinetic energy and the turbulence macroscale as the prognostic variables. The model features include a split mode time step and a sigma-coordinate transformation for the vertical grid. The bottom following sigma layers allow the model to represent accurately regions of high topographic variability. The horizontal grid uses curvilinear orthogonal coordinates and an "Arakawa C" differencing scheme. The Mellor and Yamada (1982) turbulence closure scheme is used to calculate the coefficients of vertical mixing of momentum, the vertical eddy viscosity and the eddy diffusivity of heat and salt. Density is calculated by an adaptation of the UNESCO equation of state revised by Mellor (1991).

The shelf model was implemented in the area spanning 13.80° E to 15.00° E longitude and 35.45° N to 37.10° N latitude, with a spatial resolution of $1/60° \times 1/60°$ (71×107 grid points) and 15 sigma layers (bottom following), with a concentration of levels in the surface and bottom boundary layers, and a uniform distribution in the interior. The perimeter of the model domain had a closed northern boundary at the Sicilian coast and three open boundaries at the western, southern and eastern edges. The average computational grid size was 1493 m along latitude and 1853 m along longitude. The high spatial resolution was the principal novelty of this model implementation. The model simulation was undertaken as one of the main initiatives within MFSPP to simulate shelf-scale dynamics in limited area domains. The technique depicted in Fig. 2 consisted in the two-step offline nesting of the coarse Ocean General Circulation Model (OGCM) of the Mediterranean, with two successively embedded reduced size sub-domains having increasing levels of grid resolutions. An overall downscaling ratio of 7.5 (shelf $= 3\times$ intermediate $= 3 \times 2.5\times$ OGCM) was used in order to resolve the detailed circulation over the shelf domain without the need to cover the entire large model area with the finest grid. The OGCM is based on the Modular Ocean Model (MOM), a rigid-lid model, implemented in the Mediterranean basin at 1/8° resolution, in latitude and longitude, and with 31 levels in the vertical (Pinardi and Masetti, 2000). The intermediate model was implemented in the Sicilian Channel area (Sorgente et al., 2003), and based like the shelf model on the POM, but with 22 sigma levels in the vertical.

The U.S. Navy Digital Bathymetric Database (DBDB1), with a $1/60° \times 1/60°$ resolution, was used directly for the computation of depth at each grid cell, using bilinear interpolation. The maximum depth of 1054 m to the SW of Malta limited the external courant time step to 5.71 s. Thus, the model was run with an external time step of 4 s and with internal integrations every 480 s. The shelf model was initialized from rest with (T, S) fields from the intermediate model.

The surface wind stress was obtained as a linear interpolation between monthly mean surface fluxes taken from the climatological atmospheric forcing data set derived from the ECMWF Re-Analysis data set (ERA) for the period January 1979 to December 1993, initially mapped on a regular grid with a horizontal resolution of 1 degree for the Mediterranean Sea. This coarse resolution wind field certainly presented a weak point of the model simulation. The wind stress was computed from the wind vector by the Hellerman and Rosenstein (1983) formula. Figure 3 shows that the Mistral wind from the northwest is predominant and reaches peak mean wind speeds of around 6 m/s during December and January. The wind field is weaker and less homogenous in space during summer. It should be noted that the ERA mean wind speed over a 1° square centered on the Maltese Islands is around 23% higher than the mean wind of 4.3 m/s registered at the Malta Meteorological Office from 1972–1992.

The calculation of the forcing superficial heat and salt fluxes (Korres and Lascaratos, 2003) was also based on the monthly climatological ERA data set. The solar radiation and the upward heat flux were obtained by using the bulk formulae described in Castellari et al. (1998). The evaporation rate was calculated from the Budyko-Bignami latent heat flux data set (Budyko, 1963), while the precipitation was obtained from the Legates and Wilmott (1990) monthly precipitation data. These climatological data sets were used to force the model at the surface. At the lateral boundaries, however, the model received information (temperature, salinity and velocity) by coupling to the coarse resolution model, and thus, the lateral heat fluxes may not be fully compatible to those at the surface. This discrepancy has been resolved by adopting surface boundary conditions for heat and salt that relay the surface (T, S) fields to the Med6 monthly climatology. Med6 is an enhancement of the seasonal gridded ($1/4° \times 1/4°$) Mediterranean Oceanic Data Base (MODB) historical data set (Brasseur et al., 1996), incorporating additional data from the MEDATLAS-1 initiative. This method of relaxation to climatology is common in large-scale ocean models (e.g. Cox and Bryan, 1984; Oey and Chen, 1992;

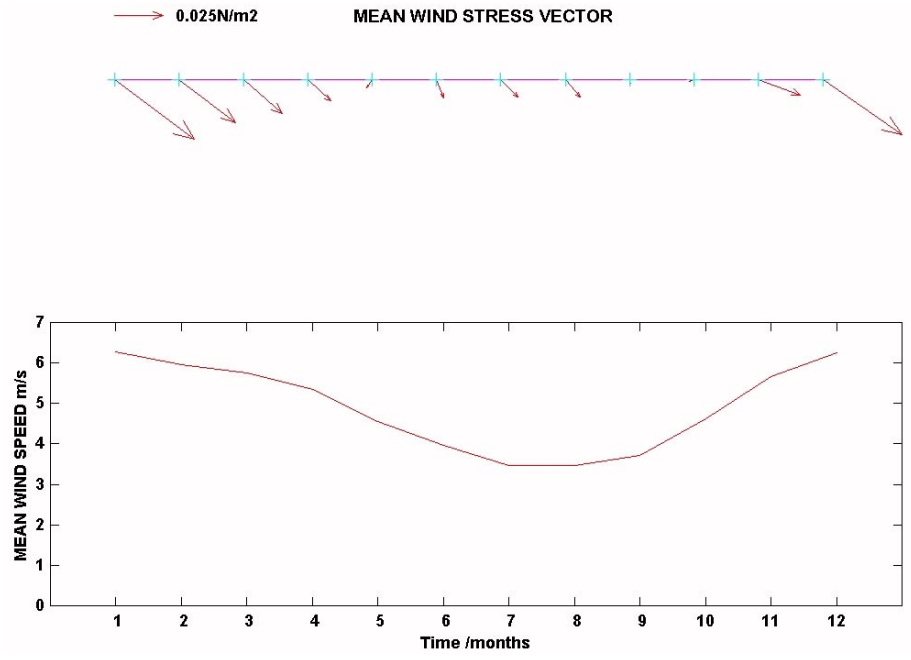

Fig. 3. **(a)** Monthly mean wind stress vector, and **(b)** monthly mean wind speed in the model domain. Data from the ECMWF re-analysis set from Jan. 1979-Dec. 1993.

Zavatarelli et al., 2002):

$$k_H \left.\frac{\partial T}{\partial z}\right|_{\eta=0} = \frac{Q_{\text{sol}} - Q_{\text{up}}}{\rho C_p} + \frac{C_1}{\rho C_p}\left(T^* - T\right) \quad (1)$$

$$k_H \left.\frac{\partial S}{\partial z}\right|_{\eta=0} = S(E-P) + C_2\left(S^* - S\right) , \quad (2)$$

where Q_{sol} and Q_{up} are the solar radiation and the upward heat flux, E is the evaporation rate, P is the precipitation, ρ is the density and C_p is the specific heat capacity at constant pressure. C_1 and C_2 are the heat and salinity flux correction relaxation constants, respectively. T^* and S^* are the monthly averaged climatological sea surface temperature and salinity, while T and S are the model's first level temperature and salinity, respectively.

The open boundary lateral conditions were provided through one-way nesting to the Sicilian Channel coarse model. The nesting of temperature, salinity and velocities (total and barotropic) was necessary, in order to transfer values from the coarsely spaced grid to the finely spaced grid at the location of the boundary regions. At each connecting boundary the mapping of the fields from the coarser to the finer grid was based on a bilinear interpolation with a momentum conservation constraint (Zavatarelli et al., 2002). The 10-day averaged fields from the intermediate model were interpolated in space over the higher resolution grid and linearly in time at each time step through an off-line, one-way nesting. The internal and external velocities to the boundary were directly specified from the coarse resolution model. In this specification the mass transport at each open lateral boundary was constrained to be equal to that on the same boundary from the coarse model:

$$\int_{l_1}^{l_2}\int_{h_{\text{high}}}^{\eta} U_{\text{total}}^{\text{high}} = \int_{l_1}^{l_2}\int_{h_{\text{coarse}}}^{\eta} U_{\text{total}}^{\text{coarse}} , \quad (3)$$

where U is the coarse grid total velocity field, U is the interpolated velocity field, h_{coarse} and h_{high} are the respective bathymetries of the coarse and high resolution grid model. This condition was imposed at each internal time step and guaranteed an exact compatibility between the high resolution fields and the original coarse model values on the lateral boundaries. The external velocity at the lateral boundaries was recalculated by a vertical integration of the adjusted total velocity, and assumed constant in the time interval between two successive internal integrations. The free surface elevation was not nested (zero gradient boundary condition), while an upstream advection was used for temperature and salinity:

$$\frac{\partial(T,S)}{\partial t} + U\frac{\partial(T,S)}{\partial x} = 0 . \quad (4)$$

In the case of outflow through the open boundaries, temperature and salinity were prescribed from the coarse model.

The one-way coupling with the intermediate model was achieved by interpolating 10-day mean values of T, S, and normal components of U and V from the 3rd year of the climatological experiment of the Sicilian Channel intermediate model. The shelf model grid was nested into the coarse model grid (Fig. 4) in such a manner as to ensure spatial compatibility on the "Arakawa C" grid of intermediate model normal velocities with the U-component shelf model velocities at $I = 2$ on the western boundary, the V-component

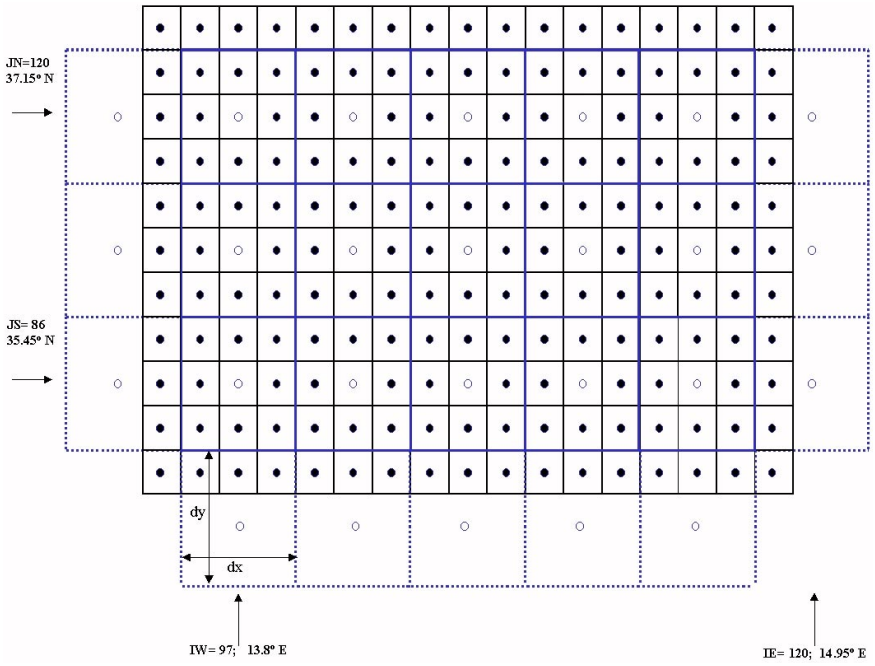

Fig. 4. Details of the coupling between the embedded shelf model fine grid (•) and the coarser intermediate model grid (○).

shelf model velocities at $J = 2$ on the southern boundary, and the U-component shelf model velocities at $I = IM$ on the eastern boundary, respectively.

The fields at the open boundaries and the atmospheric forcing at the air-sea interface have been applied on a repeating "perpetual" year cycle for three years when a steady model simulation was reached.

4 Model results

The shelf model started from 1 January with integrations running for three successive years, using the surface and lateral boundary conditions as described in the previous section. The simulated circulation in the Malta platform area presented in this work refers to the third year of the "perpetual" run of the model, with direct forcing by the ERA climatological fluxes. Following the indications of sensitivity experiments, an optimal value of $5\,m^2s^{-1}$ was adopted for the horizontal kinematic viscosity which was kept constant over the whole model domain. This was 10 times smaller than the value used for the coarse grid model. Such a small value for this parameter was necessary in order to bring to evidence the mesoscale field pertinent to the modelled domain. In the present study, the two largest islands (Malta and Gozo) of the Maltese archipelago were taken to be connected, since the grid resolution of the model does not permit the accurate representation of the separating channel.

The model results presented in this work are described by time series plots of various parameters (Figs. 5, 7 and 8), horizontal sections of (i) sea surface elevation (Fig. 11), (ii) velocities (Figs. 10, 14, and 15), and (iii) temperature and salinity (Figs. 9 and 14), as well as by meridional sections of temperature, salinity and total velocity components (Figs. 12 and 13). The horizontal velocities are plotted at 30 m, in order to view the mean surface circulation without the effect of the Ekman contribution. The plotting of temperature at 5 m depth provides better compatibility with satellite-derived sea surface temperature images. The vertical section is taken along longitude 14°20′ E to coincide with the dividing line between Malta and Gozo, cutting across the Gela Sicilian basin, and meeting that part of the Sicilian coast which appears from satellite data to be a focal starting location for upwelling events.

The seasons are represented by Julian days 1–90 for winter, 91–180 for spring, 181–270 for summer and 271–360 for autumn, respectively.

4.1 Model assessment and validation

The total kinetic energy has been used as a diagnostic to monitor the stability of the model which quickly acquires a repeating seasonal cycle after the second year of integration (Fig. 5a). The same can be inferred from the basin mean temperature and salinity (Figs. 5b, c). In order to quantify differences between the model results and observations, the time series of the simulated monthly averaged basin temperature and salinity have been compared with the Med6 climatological data set (Fig. 5). The skill of the model in reproducing the observed temperature and salinity fields has been further assessed by comparing the modelled T/S profiles with climatology at typical points in the model domain. The comparison for April and October is shown in Fig. 6, with profiles at locations in the middle of the Malta Channel ($IM = 35$, $JM = 65$) and to the south of Malta ($IM = 35$, $JM = 10$), respectively. In these plots the cli-

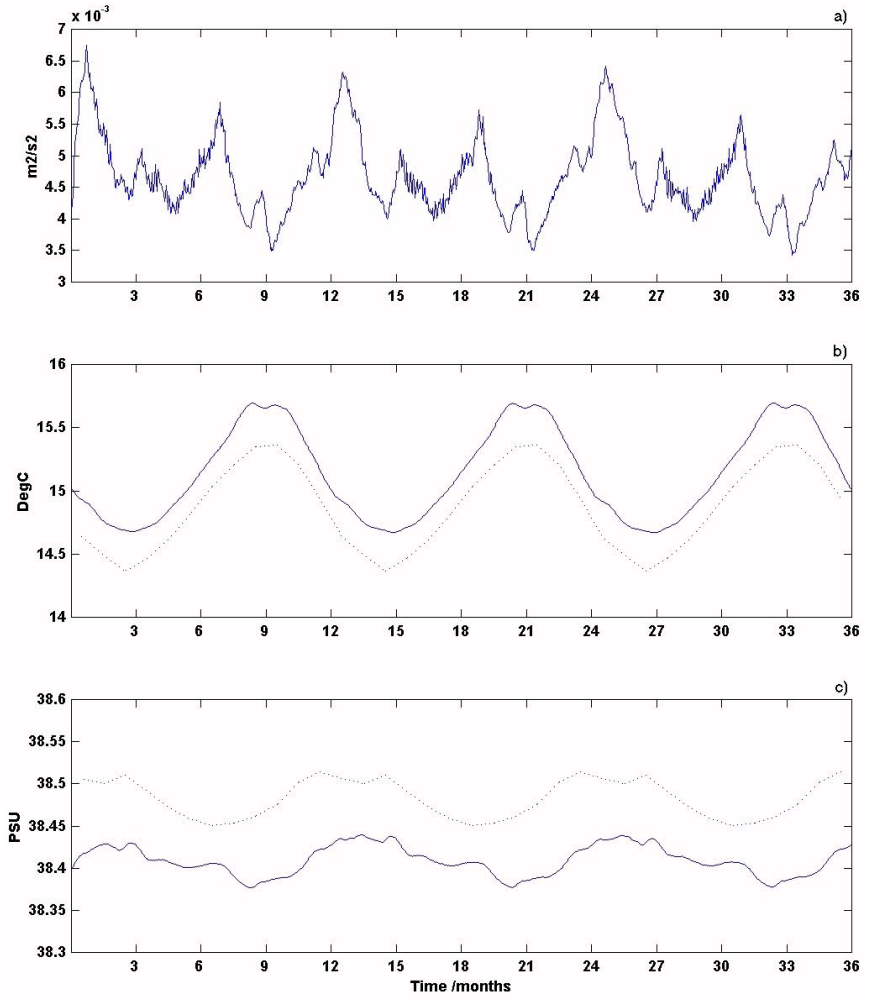

Fig. 5. Time series of **(a)** basin averaged kinetic energy, **(b)** basin mean potential temperature, and **(c)** basin mean salinity. The solid line represents the modelled values, while the dashed line represents the monthly climatological values plotted on the 15th day of the month.

matological profiles are taken from the Med6 monthly averaged fields, while the modelled profiles are taken from 10-day averaged fields calculated from day 10→20 of the month. The overall performance indicated by this kind of analysis confirmed the ability of the model to reproduce the seasonal climatological cycle and to represent well the realistic temperature and salinity fields. The modelled water column temperatures gave slightly warmer values, with differences from the climatology remaining generally less than 0.4°C, except for some cases with slightly higher temperatures close to the surface, especially in the southern part of the domain. The characteristics of the MLIW are reproduced well by the model. An average discrepancy of around 0.4 psu in the salinity, mainly at the intermediate depth, can be however noted, resulting in an overall fresher model water column. It is noteworthy that the extent of the discrepancies in both parameters, compared to their climatological values, tends to remain practically constant throughout the year from the very start of the integrations. Thus, the differences appear to be largely inherited from the initialisation fields supplied by the intermediate model. The shelf model did not, however, introduce any drift and could practically limit this discrepancy to its initial value in both cases.

The monthly climatological surface heat and water fluxes used to force the model are illustrated in Figs. 7a, b. In order to ensure that the applied heat and salinity fluxes produce sea surface temperatures and salinity values consistent with the Med6 monthly climatology, heat and salinity flux corrections were applied, as described in Sect. 3 with $C_1 = 25\,\mathrm{W\,m^{-2}{}^{\circ}C^{-1}}$ and $C_2 = 0.7$ m/day in Eq. (1) and Eq. (2), respectively. The modelled heat and water surface fluxes, together with the mean superficial temperature and salinity, are shown in Fig. 7, with a comparison to the climatological time series. The heat gain is typically high during summer and somewhat supercedes the heat loss in winter, producing a net positive simulated heat budget of $10.8\,\mathrm{W\,m^{-2}}$ compared to the climatological mean of $23.3\,\mathrm{W\,m^{-2}}$. The heat gain is highest in June, while heat losses are maximal in November. This is congruous to the seasonal evolution of the temperature in the top layer, with a range in excess of 10°C, a minimum towards March and a maximum in August. The seasonal cycle of the fresh water budget due to evaporation minus precipation ($E - P$) is characterized by low values in winter and spring, and by higher values during summer and autumn. The modelled surface water flux transitional peak in March and the accentuated increase in October are artifacts

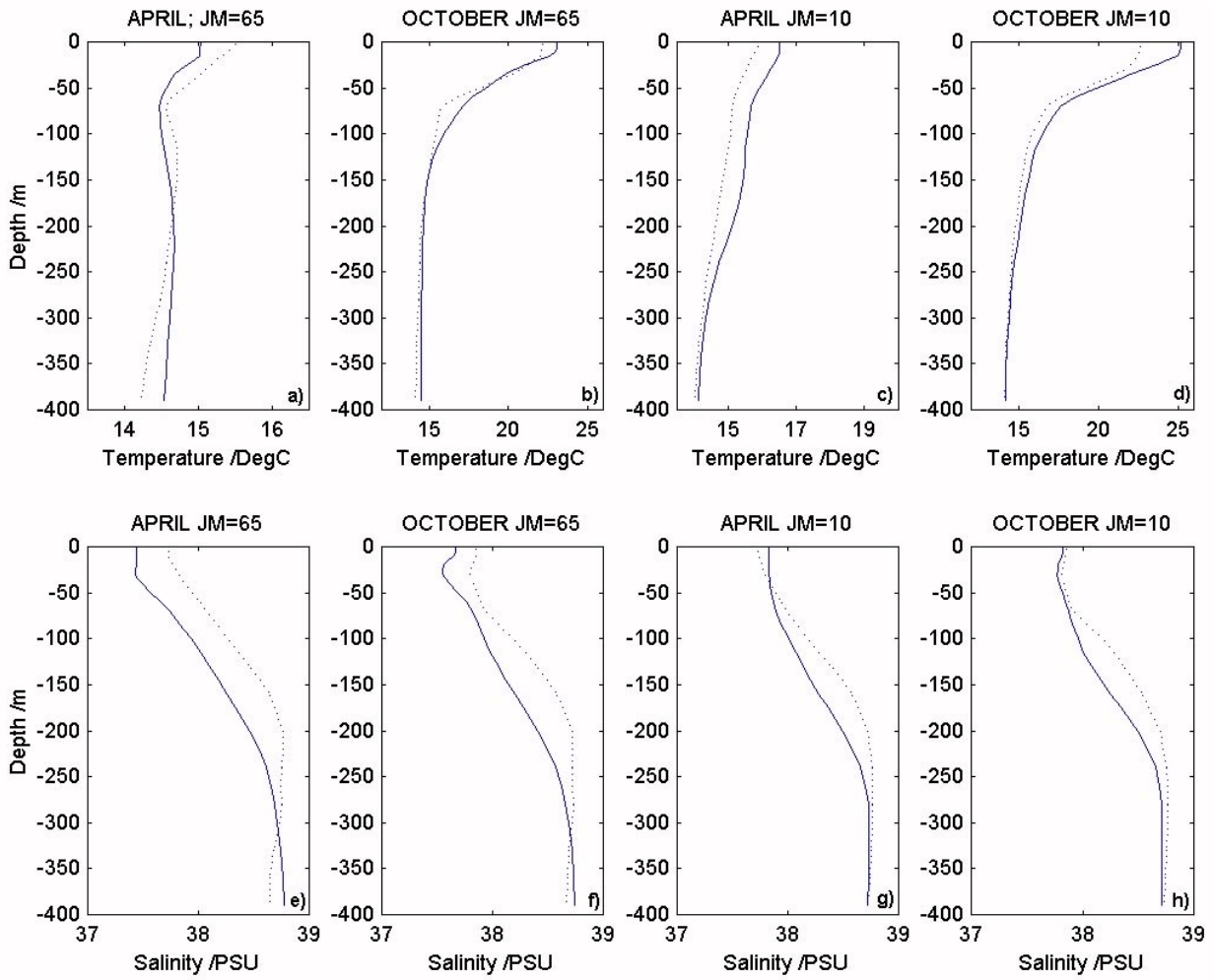

Fig. 6. Comparison between the modelled (solid line) and Med6 climatological (dotted line) temperature (a–d) and salinity (e–h) profiles at locations in the middle of the Malta Channel ($IM = 35$, $JM = 65$; (36.4° N, 14.4° E)) and to the south of Malta ($IM = 35$, $JM = 10$; (36.4° N, 14.4° E)), respectively, and at two different periods of the year (April and October). Climatological profiles are taken from monthly averaged fields. Modelled profiles are taken from 10-day averaged fields calculated from day 10→20 of the month.

and could be attributed to the mismatch between the model and climatological surface salinity. It is evident that the relaxation scheme on salinity does not work as efficiently as it does for temperature. On the other hand, the model does not introduce any drift in either parameters.

Confidence in the model's performance can also be obtained by matching the benchmark shelf scale model simulation with the outer coarse model output calculated over the inner domain. A comparison of 10-day averaged time series of key parameters between the two models (Fig. 8) has been used to quantify the robustness of the nested-grid technique used in this experiment. The correlations in the mean volume temperature (Fig. 8a), and in the eastward volume transport across the longitudinal section running along 14.4° E from Malta to Sicily (Fig. 8d), were both very high. The variation of the mean volume salinity in time is identical in the two models, except for a shift of 0.05 psu (Fig. 8b); this positive shift in the shelf simulation compensates, at least in part, for the negative discrepancy (already referred to above) of the coarse model salinity field with respect to observations. The correspondence in the flow fields has also been assessed in detail by comparing the E-W and N-S total velocity components at a set of selected depths and locations common to the two models, such as in the example in Figs. 8e and 8f for a point (36.4° N, 14.4° E) in the middle of the Malta Channel. The mean flow between the two models is very similar, with a general decrease in correlation with depth due to differences in the bathymetry resolved by the two models. Differences are also noticed especially in the summer AIS flow magnitude, which rises by around 20% in the shelf model implementation; this explains the higher mean volume kinetic energy values of the inner model (Fig. 8c). In general, these results confirmed that the shelf model can adequately replicate the general dynamics and seasonal variability of the outer model solution.

A visual match between the two models can be further

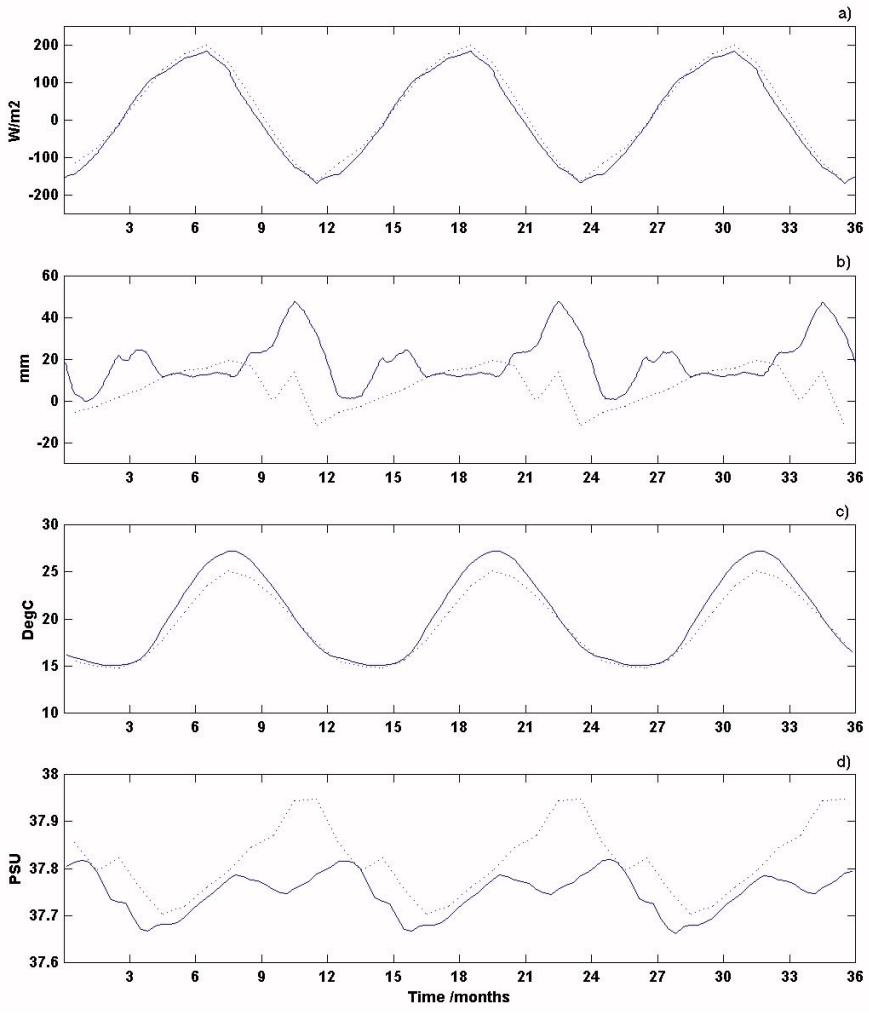

Fig. 7. Time series of surface averaged **(a)** total heat flux, **(b)** evaporation minus precipitation ($E - P$), **(c)** temperature and **(d)** salinity. Modelled values (solid line), monthly climatological values plotted on the 15th day of the month (dashed line).

made by comparing plots of horizontal fields, such as of temperature (Fig. 9), salinity (not shown) and the 2-D flow (Fig. 10). In these example plots, the temperature is at 5 m depth, while velocities are at 30 m. Values are averaged over the first ten days of January. Such comparisons are useful to verify the ability of the inner shelf model to replicate the spatial features of the outer model, as well as to assess the performance of the boundary conditions by checking for spurious signals or inconsistencies at the lateral boundaries. Moreover, they show the merit of the fine grid model in improving the resolution of the mesoscale detail. In the particular comparison made in Fig. 10, the simulated flow in the fine model replicated the same broadscale flow patterns of the outer model; however, it brought out in detail the branching and meandering dynamics of the AIS stream as it traverses the shallow shelf bathymetry, and the shorter scale eddy formations evolving and propagating close to the Maltese Islands. The general pattern of flow is very similar to that of the intermediate coarse model, but clearly contains additional detail which cannot be discerned in the coarse model solution. Except for some unwanted noise in the north-south velocity component on the eastern boundary, the coupling appears to succeed in adequately capturing and extending the circulation features close to the nesting boundaries into the shelf model. Thus, the downscaled simulation reproduced the same dynamical features and repeated the same temporal development of the general circulation patterns produced by the coarse model. This positive assessment can be practically extended to the whole period of simulation, although the level of compatibility varies for different months.

4.2 Description of mean fields and variability

A first hand characterization of the modelled circulation can be inferred from the seasonal maps of sea surface elevation (Fig. 11). The predominant feature in the surface flow is the swift Atlantic Ionian Stream (AIS), which carries the relatively fresher water of Atlantic origin across the Malta Channel. It prevails throughout the year, but with significant seasonal variability mainly in its spatial distribution more than its strength. During winter, it follows closely the Sicilian coast up to 14.4° E longitude after which it detaches in a southeasterly direction as it progresses over the shallower parts of the shelf. In summer it is broader, fanning out in

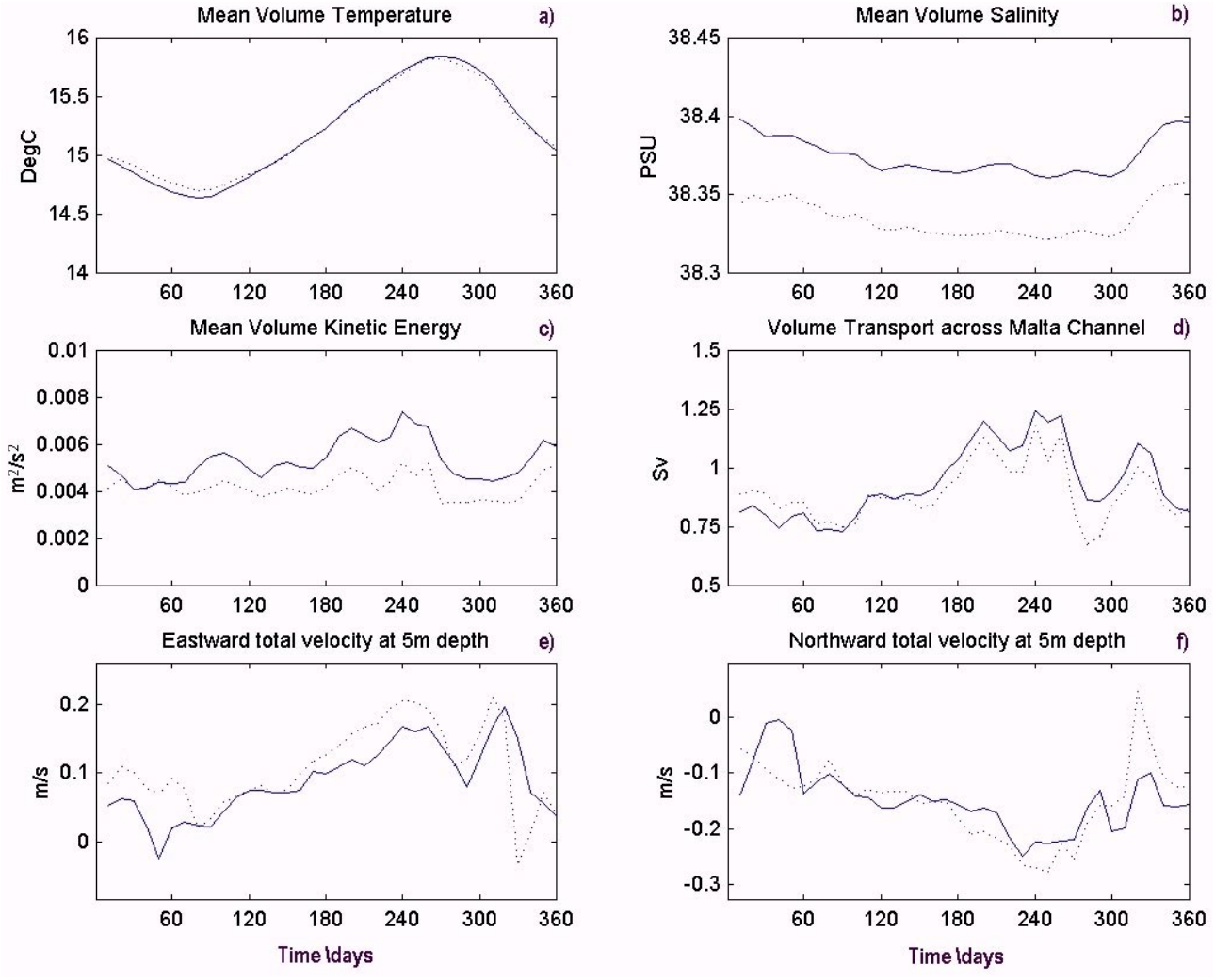

Fig. 8. Comparison between the inner shelf scale (solid line) and outer coarse scale (dotted line) models by 10-day averaged time series of mean volume **(a)** temperature, **(b)** salinity and **(c)** kinetic energy calculated over the inner model domain; **(d)** volume transport across the vertical section running along 14.4° E; **(e)** E-W and **(f)** N-S total velocity components at 5 m depth taken from the model output at a common point in the middle of the Malta Channel (36.4° N , 14.4° E).

horizontal extent and shifting its main stream axis southwards, cutting across the Maltese Islands. Part of the stream is re-circulated in spring by an anticyclonic circulation to the northwest of the Maltese Islands over the Sicilian Gela basin. The stream is also accompanied by a persistent barotropic cyclonic circulation south of the eastern tip of Sicily, which is enhanced during summer and occurs in association to density gradients produced by the intrusion of cooler and more saline water from the Ionian. An anticyclonic pattern on the southwestern extremity of the model domain persists during the winter months, bringing relatively warmer and more saline water from the south; it shifts southwards and fades out of the model domain in late spring. It is noteworthy that the pressure gradient attains its maximum in summer rather than in winter when the wind forcing from the northwest is most intense. This apparent paradox is treated later on in the section where the Sicilian upwelling phenomenon is dealt with in detail.

4.2.1 Water mass structure

The meridional sections of temperature and salinity along latitude 14°20′ E, plotted from 10-day averaged fields in January, April, July and October (Fig. 12), and the 2-D horizontal plots in Fig. 14, are used to present the water mass structure and seasonal development of the hydrography. Robinson et al. (1996) have identified seven water masses in the northern area of the Strait of Sicily and the northwest Ionian Sea. Starting from the Modified Levantine Intermediate Water (MLIW) at the bottom, the successive overlying layers consist of the Transitional, Fresh, Mixed, Modified Atlantic, Upper and Surface water masses. Traditionally, the

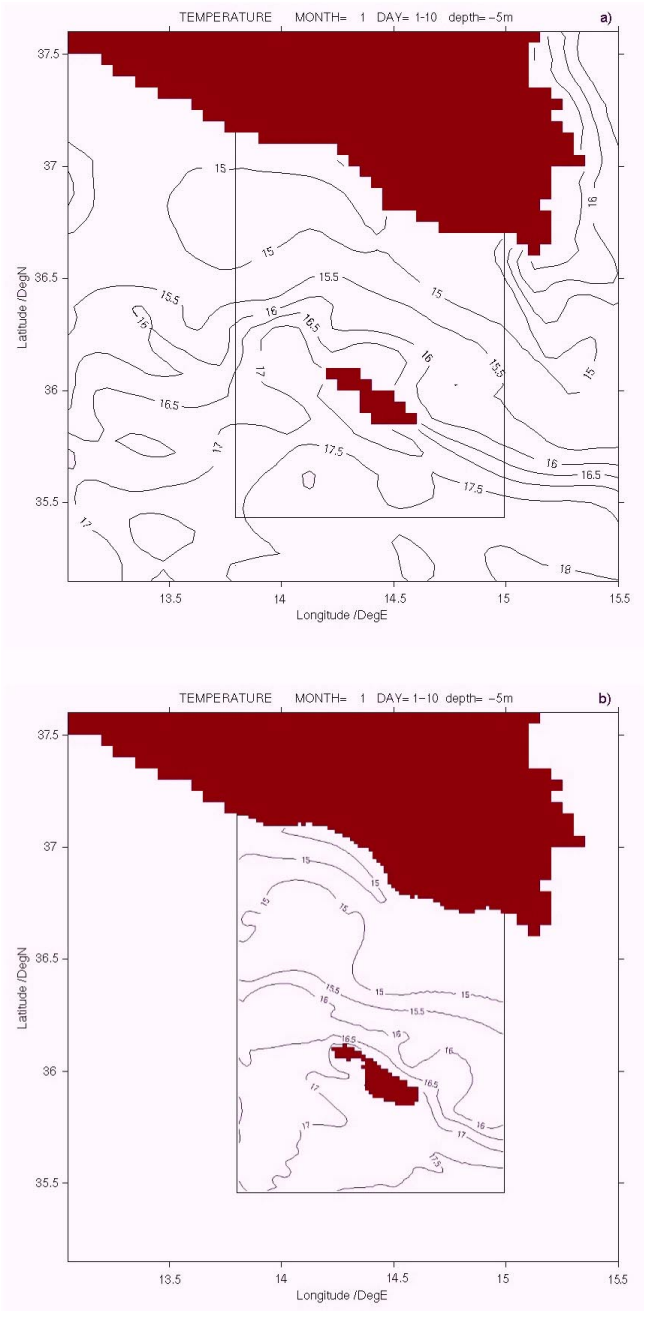

Fig. 9. Comparison of the 10-day averaged temperature horizontal field at 5 m depth in January simulated by **(a)** the coarse resolution model and **(b)** the benchmark high resolution shelf model.

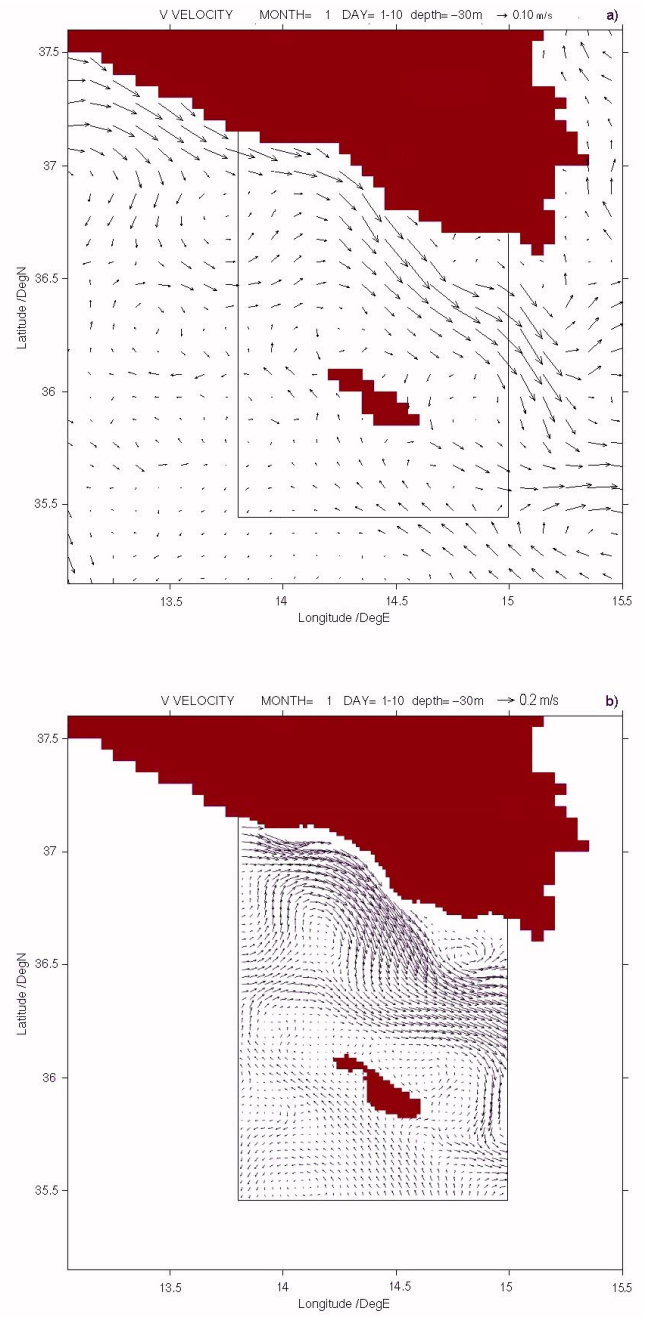

Fig. 10. Comparison of the 10-day averaged 2-D flow field at 30 m depth in January simulated by **(a)** the coarse resolution model and **(b)** the benchmark high resolution shelf model.

three main water masses are more simply described by the upper layer Modified Atlantic Water which enters through the Sicily Channel as an extension of the north African Algerian coastal current, the transitional layer and the deeper MLIW moving towards the west.

The strong seasonal variability in the salinity of the surface MAW, as well as in the thickness of this layer, is well evidenced by the model simulations. In consequence of the sustained surface evaporation caused by the increase in solar heating, the upper water layer in summer is characterized by a maximum salinity (reaching an average of 37.8 psu to the south) and a high temperature ranging between 20°C to 27°C from north to south (Fig. 12c). The underlying water has a lower salinity of the order of 37.4 psu, thus presenting, especially in the north, a salinity minimum with respect to the surface water. Its temperature is between 16°C and 19°C. In mid-July this water of Atlantic origin appears as a well-defined subsurface core, centered along 36.6° N of latitude at an average depth of 20 to 60 m (Fig. 12f). This agrees with the general situation in the broader Sicily Channel area,

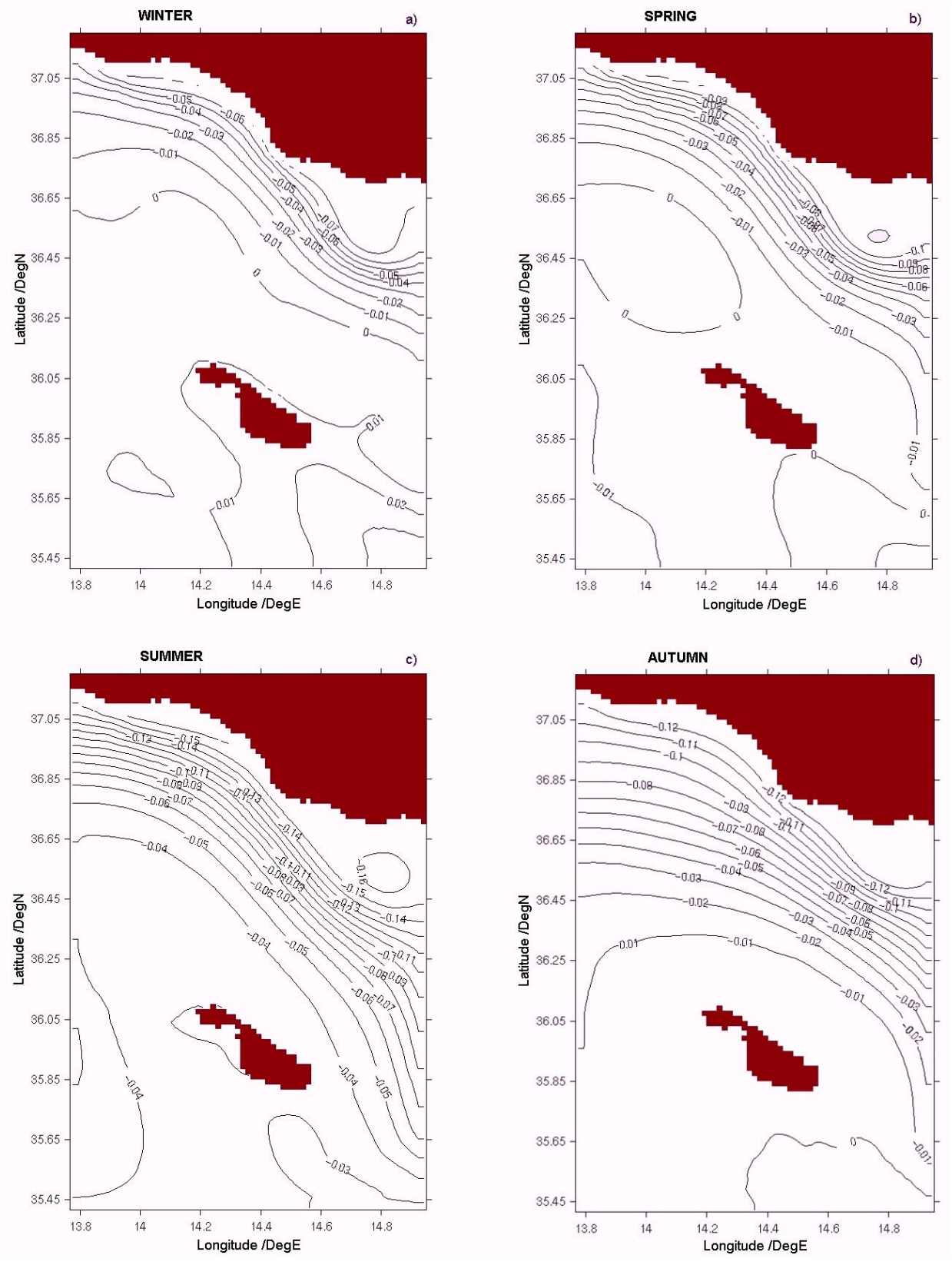

Fig. 11. Mean seasonal free surface elevation field in the model domain for **(a)** winter, **(b)** spring, **(c)** summer and **(d)** autumn.

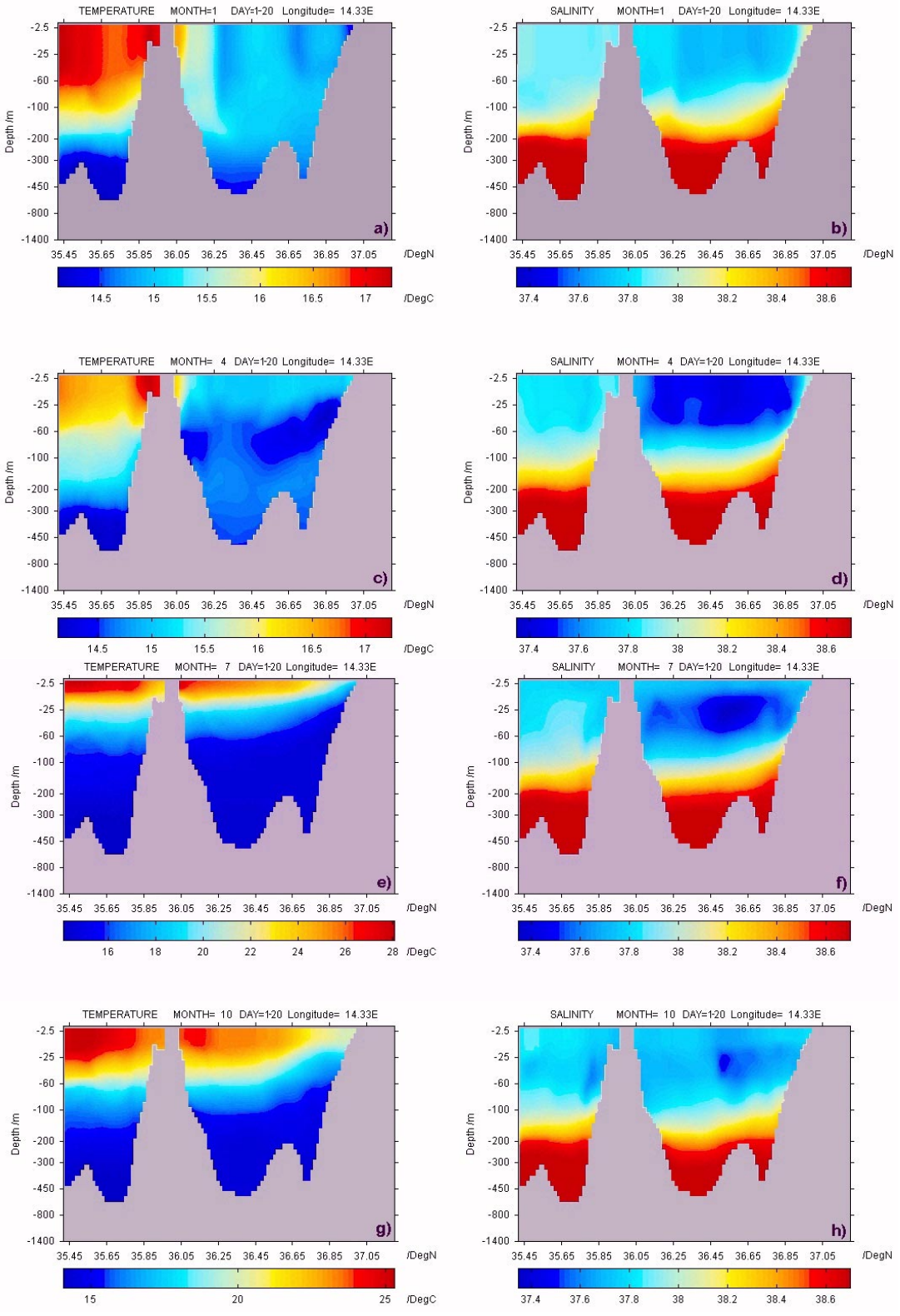

Fig. 12. Vertical sections of ten-day averaged temperature and salinity for the second third of January **(a)**, and **(b)**, and for the second third of April **(c)** and **(d)**. The section runs from south to north along longitude 14°20′ E. Plotting of velocity vectors is done only at every odd grid point. Vertical sections of 10-day averaged temperature and salinity for the second third of July **(e)** and **(f)**, and for the second third of October **(g)** and **(h)**. The section runs from south to north along longitude 14°20′ E. For plotting of velocity vectors is done only at every odd grid point.

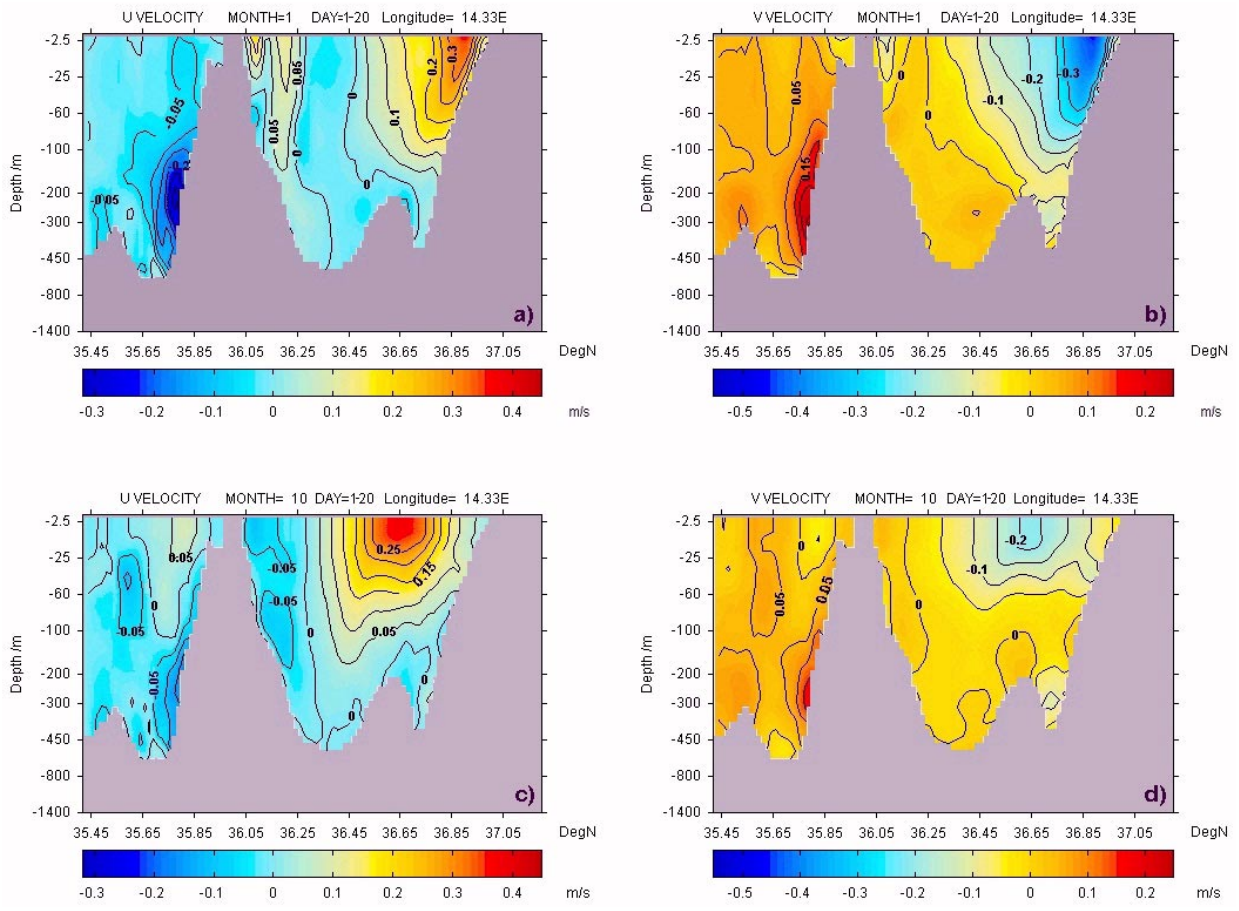

Fig. 13. Vertical sections of 10-day averaged east-west total velocity components and north-south total velocity components for the second third of January **(a)** and **(b)**, and for the second third of October **(c)** and **(d)**. The section runs from south to north along longitude 14°20′ E. In (a) and (c) positive velocities are directed towards east and negative velocities directed towards west. In (b) and (d) positive velocities are directed towards north and negative velocities directed towards south.

where the signature of the MAW is seasonal and represented by a salinity minimum situated at about 50 m in depth during summer and near the surface during winter (Wust, 1961; Manzella, 1988). This core is gradually eroded as the winter season is approached, and strong surface cooling and vertical mixing come into action. A single homogeneous water mass is formed in the Malta Channel up to a depth of 100 m with temperatures around 15°C; to the south the upper layer temperatures are around 2°C higher (homogeneous up to 60 m) mainly due to the advection of warmer water from the south (Fig. 12a). The Maltese Islands are thus, very often situated within a frontal zone, with appreciable differences in temperature between the northern and southern shores. In early spring the presence of the fresh MAW starts to regain its evidence between Malta and Sicily, but its temperature in the upper layer remains greatly conditioned by surface forcing.

A transition stable water layer resides between around 100 m and 200 m depth with an average salinity of 38.2 psu and an average temperature of 15.5°C (Fig. 12). This intermediate water is more saline than the overlying water masses and is the result of mixing of the Atlantic water with the deeper more dense water. The characteristics of this layer are rather persistent throughout the year except that it is less thick in winter (Fig. 12a). In agreement with the MEDATLAS I data set the deeper water mass resides below 250 m in winter and has a temperature decreasing with depth from 14.7°C to 14°C with a uniform salinity of around 38.75 psu. This water mass is identified as the MLIW and is practically absent over the Malta shelf areas with depths shallower than 100 m. It presents a maximum salinity in the western and southwestern approaches of Malta. The renewal time of the total MLIW in the channel has been estimated to be around 9 months (Manzella, 1988), which is long enough to explain the fairly constant salinity over the annual cycle.

4.2.2 Circulation

The variability of the simulated currents is investigated by means of vertical sections of the latitudinal and meridional components of the total velocity (example plots for January and October in Fig. 13), together with horizontal plots of 10-

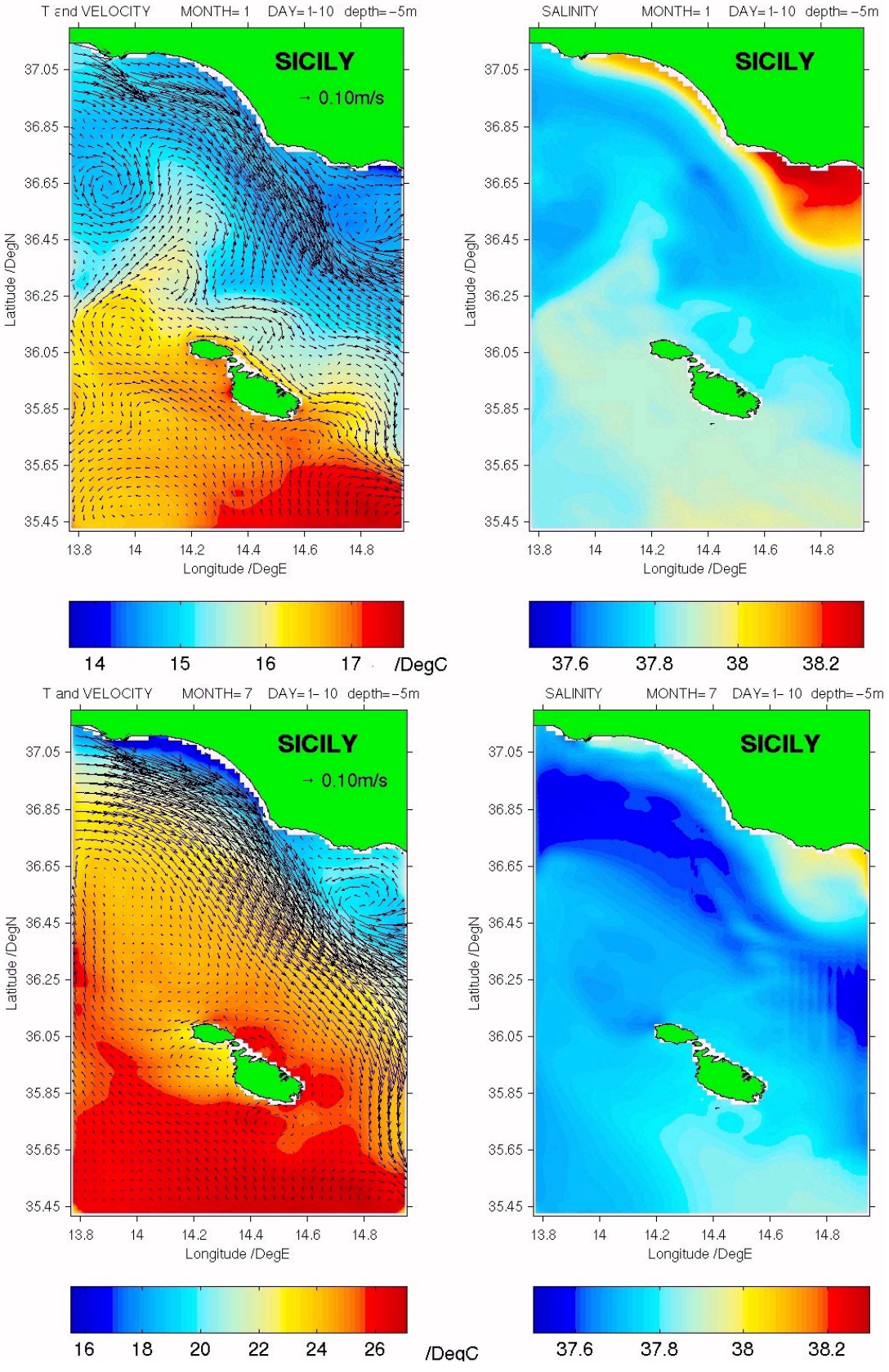

Fig. 14. Ten-day averaged temperature **(a)** at 5 m and total velocity horizontal fields at 30 m and **(b)** salinity at 5 m for the second third of January, and of July **(c)** and **(d)**. Plotting of velocity vectors is done only at every odd grid point.

day averaged flow fields (example plots for January and July in Fig. 14). In Fig. 13 the plots are along a section running across the Malta Channel from the Maltese coast to Sicily along longitude 14°20′ E. The contours join points of equal total velocity eastward (Figs. 13a, c) and northward components (Figs. 13b, d). They furnish a view of the vertical structure of the flow. In combination these plots put in evidence the skill of the model to replicate the hydrodynamics in the area while furnishing a detailed 3-D view of the circulation and a description of its variability.

The phenomenology and variability of the upper layer mean flow is dictated by the Atlantic Ionian jet stream moving eastward across the domain, and the strong upwelling activity adjacent to Sicily. The surface coastal current associated with the upwelling system flows southeastward following the Sicilian coast and merges with the AIS, forming an intense core centered over the shelf area during winter and spring. As indicated from Fig. 13, the peak surface horizontal velocities reach values of around 0.4 m/s, being slightly weaker in winter. The flow has a quasi-barotropic nature in the top layer, but is accompanied by strong velocity shears in the bottom boundary layer and along its lateral boundaries as it extends horizontally up to a latitude of 36.4° N, and vertically beyond the Sicilian shelf break. It practically maintains the same intensity throughout the year. In winter and spring it remains close to the coast, and largely exits the model domain close to 36.3° N of latitude along a path that almost cuts across the isobaths (Fig. 14). During summer the core velocities are slightly high, but the horizontal extent is wide and the stream practically fills the whole meridional extent of the Sicilian basin and Malta platform area. Its path takes a more southward oriented diversion and tends to follow more the bathymetry. Its axis is progressively shifted southwards in late summer, culminating into a complete detachment in October; the flow is then restricted to a reduced core residing in the upper 30 m and is no longer bound to the coast and bathymetry. Thus, the seasonal variability of the flow is mainly characterized by its spatial extent, position and path rather than its intensity.

At depth the path and seasonal evolution of the MLIW can also be followed in Figs. 12, 13 and additional 2-D plots at various depths (not shown). A predominant, well-defined northwesterly flux of saline MLIW flowing over the slope to the south of Malta exists in winter, with its main core centered at around 280 m and with a vertical extent of more than 200 m. It is characterized by a very stable temperature of around 14.8°C and a salinity of 38.8 psu, in close agreement with values quoted in the literature (Warn-Varnas et al., 1999; Wust, 1961). It attenuates somewhat in spring, moving to a slightly deeper position in summer when it becomes even weaker. This is in agreement with the long-term time series of currents in the Sicilian Channel by Grancini and Michelato (1987), which indicated that the Levantine water transport exists at smaller depths during winter and is 2–3 times stronger than during summer.

The model results also show the presence of the AIS meandering along the Malta Channel with different mesoscale extensions and dynamic patterns associated with the instability of the stream as it moves eastward across the shallower shelf. Along its path the AIS is known to be accompanied by various mesoscale structures in the form of current meanders, eddies and filaments (Lermusiaux, 1999). The formation and characterization of these mesoscale patterns can be mainly connected to internal dynamical processes. They are produced as a result of flow interaction with topography and greatly affected by transport variations in the general circulation. Their evolution, propagation and spatial development is furthermore controlled by the hydrographic structure of the water body and modified by the synoptic scale atmospheric forcing fluctuations. The low temporal resolution of the surface forcing fields does not, however, permit this atmospheric component to be fully expressed. Nonetheless, the model gives evidence to a significant mesoscale activity over the model domain, implying the importance of the intrinsic dynamical instabilities triggered by the interaction of the circulation with the bathymetry, and the land emergence constituting the Maltese Archipelago.

The model results have also been viewed by animating a sequential series of 10-day averaged 2-D plots of surface circulation fields covering a full year of simulation. The animation provides a simple and vivid method of viewing and studying the temporal development of the flow dynamics in the area. It shows the predominant characteristic of the circulation in the vicinity of the Maltese Islands, consisting in the evolution and propagation of mesoscale eddies which form mainly as a result of the impact of the shallowing bathymetry and the proximity of land on the AIS flow. Besides trapping water and particulates, these eddies have associated vertical motions that influence phytoplankton biomass distributions and thus, bear important links to biological processes, in particular, to the location of fisheries (Wolanski, 1995). Moreover, the proximity of the islands to the shelf break exposes the southern coast to upwelled water (Fig. 14c), especially during summer when an anticyclonic circulation becomes established in the area separating the souteastern tip of Gozo from Malta, a favourite location to fishermen.

4.2.3 Upwelling

The shelf on the southern coast of Sicily is a main upwelling area of the Mediterranean. It is favoured by the northwesterly gusts that are numerous and can be particularly strong at any period of the year. It brings to the surface cool water that is then advected away for large distances away from the coast. Although the upwelling events peak in summer and early autumn, they tend to be toward year round, with a period of attenuation in spring. Thus, the oceanic ecosystem in this zone is not limited to a single productivity event per year, and primary production is significantly greater both in period and rate.

The vertical sections of the model temperature and salinity are useful to study and to describe the physical processes responsible for the mesoscale variability of the hydrophysical structure in the upwelling zone. The inclination of the

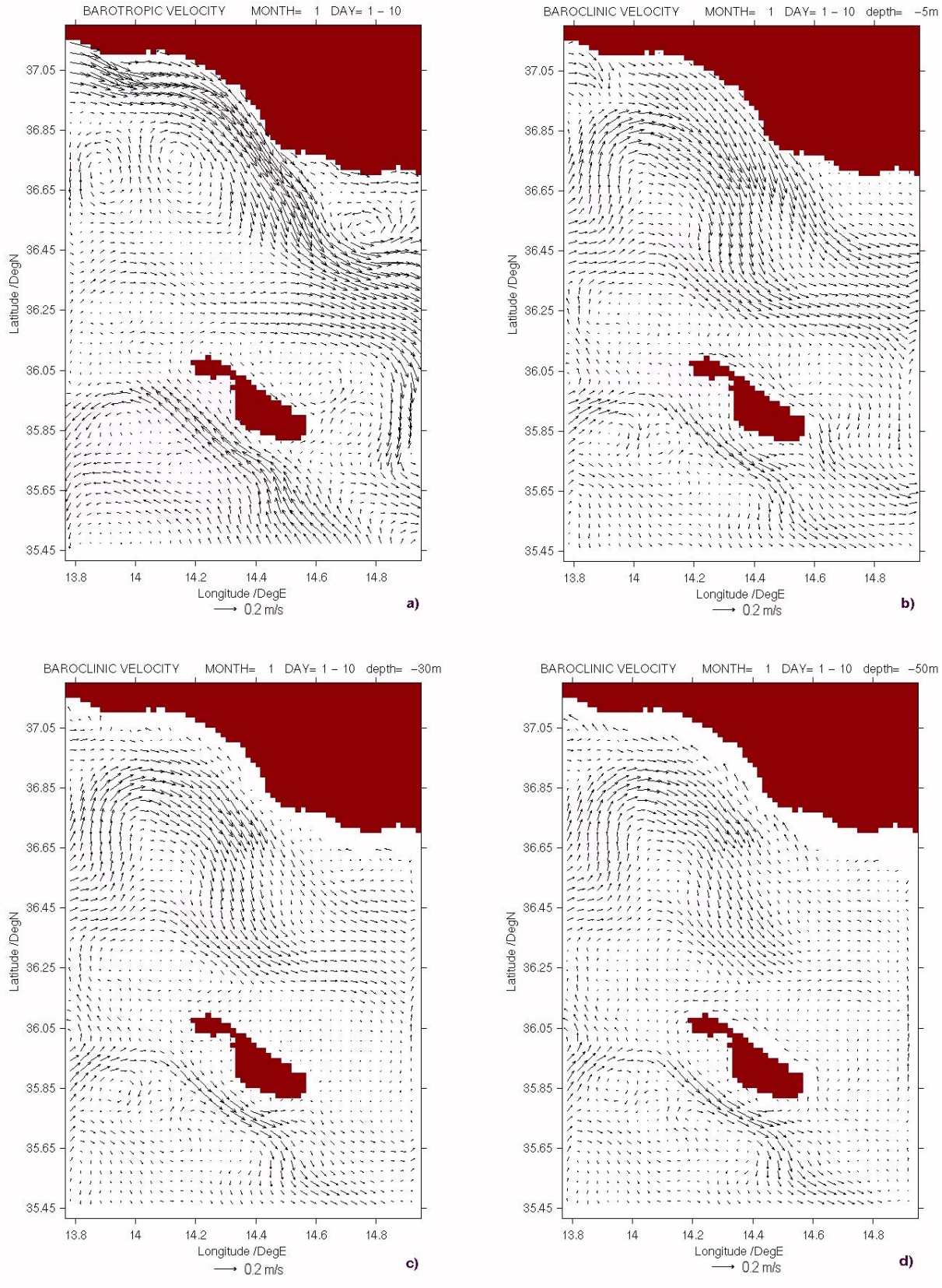

Fig. 15. Horizontal fields of **(a)** barotropic velocity, and baroclinic velocity at **(b)** 5 m, **(c)** 30 m and **(d)** 50 m depth, for the first ten days of January. Plotting is done only at every odd grid point.

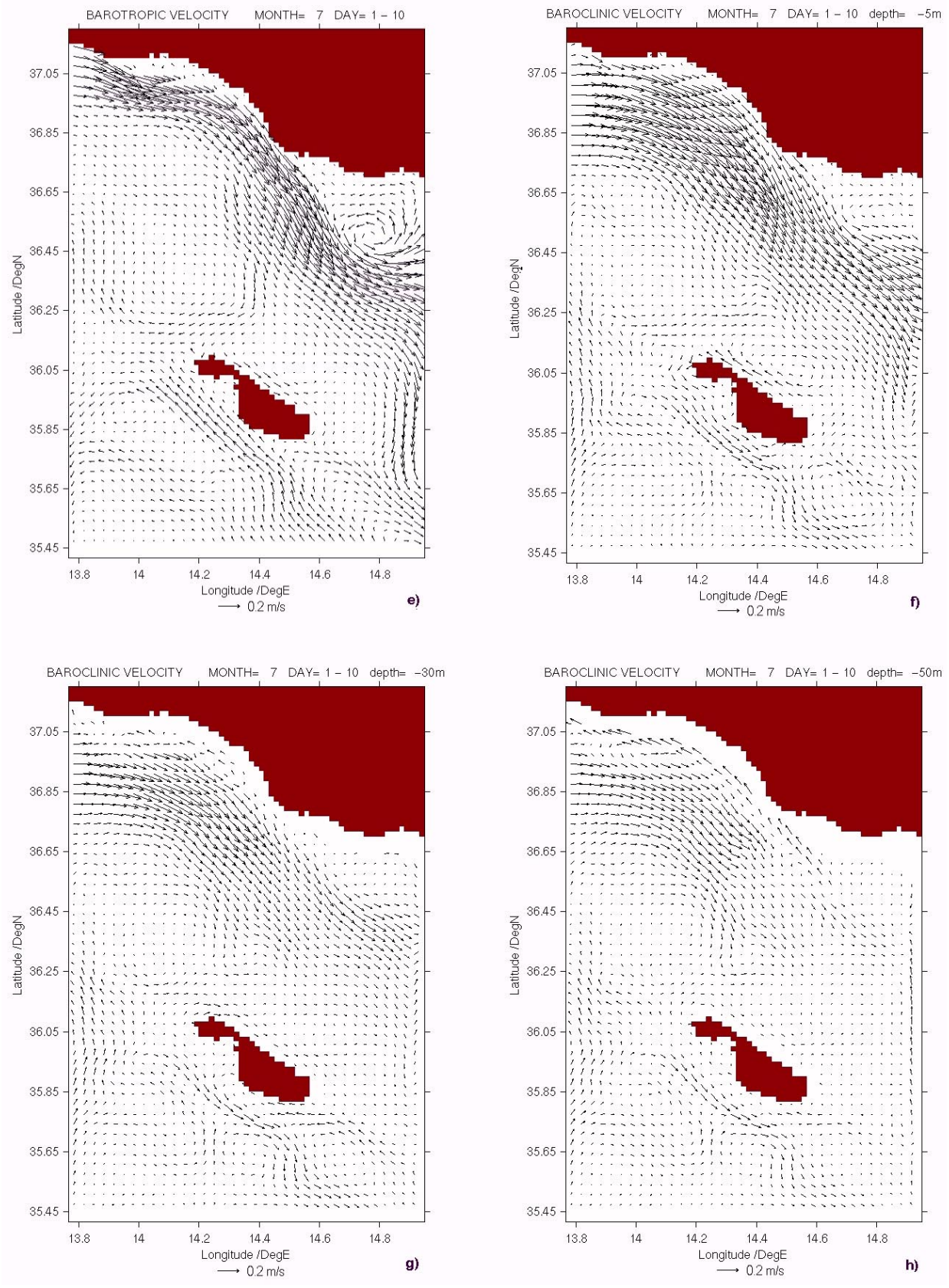

Fig. 15. Continued: Horizontal fields of **(e)** barotropic velocity, and baroclinic velocity at **(f)** 5 m, **(g)** 30 m and **(h)** 50 m depth, for the first ten days of July. Plotting is done only at every odd grid point.

isotherms confirms that upwelling persists throughout the year, but is most evident in summer and early fall when the water column becomes well stratified and the thermocline is able to surface close to the southern Sicilian coast. The upwelled water originates from depths that do not exceed 80 m (Fig. 12c), but the cross-shelf circulation associated with coastal upwelling is able to somewhat extend southwards into the Malta Channel (Figs. 13 and 14), being eventually caught by the advective influence of the AIS. This is in agreement with IR satellite imagery analysis, which gives upwelling widths of around 100 km and maximal horizontal temperature contrast and gradients across the upwelling front of 3°C and 0.4°C/km in the period August–October (Kostianoy et al., 1998). The upwelling process is not able to break down the shelf stratification which remains in evidence, except very close to the coast, where the mixed layer is able to reach the bottom. It is somewhat peculiar that, as noted also by Kostianoy et al. (1998), the upwelling is most evident in summer rather than in winter when the wind stress is some three times stronger.

Figure 15 gives an interesting decomposition of the characteristic barotropic and baroclinic components of the mean flow field in the first ten days of January and July, respectively. The barotropic wind-driven contribution to the swift flow in proximity of the Sicilian coast is very stable seasonally. On the other hand, the baroclinic component carries an evident seasonal signal, being spatially more widespread and variable in winter, performing a large meandering movement, while it is more intense and focussed in summer. This component of the AIS appears to be driven by mechanisms external to the model domain, possibly resulting from intrabasin differences. The surface expression to its summer intensification is expected to be in the form of an enhanced sea level gradient, tending to re-establish geostrophic equilibrium. This gives a clue on how to resolve the seasonal cycle of the upwelling system. If the flow along the southern coast of Sicily were to manifest itself solely in response to wind forcing, one would expect higher gradients in elevation during winter. On the contrary, upwelling is stronger in summer when the wind field is weaker and blows less frequently from the favourable northwesterly direction. A plausible explanation that emerges is that upwelling during summer and early autumn is favoured by the geostrophic adjustment of the sea surface in response to an intrinsic strengthening of the AIS flow, thus leading to a lowering of the sea surface profile towards coast. In combination with the presence of the stratification close to the surface, upwelling events hence become easily triggered in summer, even with moderate surface wind forcing.

5 Summary and discussion

The results presented in this paper showed that the two-step coupling of the large-scale Mediterranean Ocean General Circulation Model to an embedded intermediate-grid primitive equation ocean model and subsequently, to a higher resolution shelf-scale implementation with three open boundaries and monthly surface forcing, was able to furnish an adequate downscaled description of the seasonal climatological cycle in the area of sea around the Maltese Islands and the Malta Channel. The one-way, off-line nesting procedure connected the models with an updating of the lateral boundary conditions using 10-day averaged fields. The outer model was integrated and provided information to update the open boundary conditions of the inner model. A conservation constraint was imposed on the interpolated and averaged transports at each lateral connecting boundary. The method was found to be computationally efficient and sufficiently robust to transmit information across the connecting boundaries without excessive distortion.

The model was able to reproduce, with the right order of magnitude, the salient dynamical features in the area, providing in addition an insight into their 3-D phenomenology and their seasonal variability. The model also replicated the water mass composition in the region, and captured the alterations in the hydrophysical structure through the seasons. The general thermohaline circulation has been expressed in the model by the upper layer fresh water southeasterly flow along the AIS and the counterflow at depth of the more saline MLIW along the slope to the south of the Maltese Islands. The progression of both flows across the model domain was greatly influenced by the topography. Their seasonal variability appeared to be largely controlled by remote intrabasin forcing. The MLIW flow was found to exist at smaller depths in winter when it is also much stronger. The spatial and temporal variability in the AIS flow was expressed mainly in its baroclinic component. Its intensification during summer and early autumn carried an associated sea surface height gradient response that favoured, in combination with the presence of a strong upper layer stratification, an enhanced coastal upwelling activity.

The strong eddy field component of the circulation in the area depends both on internal dynamical processes, as well as on the influence of the synoptic scale atmospheric forcing (Pinardi and Masetti, 2000). The model grid was sufficiently fine to admit a correct representation of the mesoscale signals, but the low temporal resolution of the surface forcing fields places a limitation on the model from capturing the full mesoscale variability. Nonetheless, substantial eddy field structures were generated by the model both along the AIS and over the shallow bathymetry, in particular around the Maltese Islands. This showed that internal nonlinear dynamics plays an important role in the mesoscale eddy field structure.

The model did not, however, appear to significantly generate any of the filament structures that appear on thermal IR images along the advection paths of upwelled water. This is probably linked to the inability of the model to produce sufficiently strong temperature gradients that are inducive to such surface features. Further sensitivity studies are necessary to assess the extent to which this depends on the fine tuning of the dispersion coefficients or on the frequency of the atmospheric forcing. It is also necessary to check the robustness

of the model to the positioning of the open lateral boundaries and its response to higher resolution atmospheric forcing.

This work has initiated the basis for a nested shelf-scale hydrodynamical model implementation with active thermodynamics in the stretch of sea covering the Malta platform and the surrounding slope area. The model promises to achieve an efficient downscaling of the large-scale circulation with a reproduction of the major dynamical features of the known climatological circulation in the area. Further tests are envisaged to refine the methodology with improved initialisation procedures, to use higher resolution atmospheric fields in both space and time, and to improve the skill of the simulations at the coastal scale with finer outer/inner model grids. This will prepare the way towards achieving near real-time shelf/coastal scale forecasts within the next phase of MFSPP.

Acknowledgements. This work was conducted in the framework of the Mediterranean Forecasting System Pilot Project (MFSPP). We acknowledge the support of the European Commission Marine Science & Technology (MAST) Programme under contract MAS3-CT98–0171. We also thank the anonymous reviewers for their helpful criticisms and advice.

Topical Editor N. Pinardi thanks W. Hanmza and another referee for their help in evaluating this paper.

References

Blumberg, A. F. and Mellor, G. L.: A description of a three-dimensional coastal ocean circulation model, in: Three dimensional coastal ocean models, Coastal Estuarine Science, (Ed) Heaps, N. S., AGU, 1–16, 1987.

Brasseur, P., Beckers, J. M., Brankart, J. M., and Schoenauen, R.: Seasonal temperature and salinity fields in the Mediterranean Sea: Climatological analysis of a historical data set, Deep Sea Res., 42(2), 159–192, 1996.

Budyko, M. I.: Atlas of the heat balance of the Earth, Glabnaia Geofiz. Observ., 1963.

Camilleri, M.: Controlling fishing effort on demersal resources in the Maltese Fisheries Management Zone, Internal Report of the Dept. of Fisheries and Aquaculture, 2000.

Castellari, S., Pinardi, N., and Leaman, K.: A model study of air-sea interactions in the Mediterranean Sea, J. Mar. Sys., 18, 89–114, 1998.

Champagne-Philippe, M. and Harang, L.: Surface Temperature fronts in the Mediterranean Sea from infrared satellite imagery, in: Hydrodynamics of semi-enclosed seas, (Ed) Nihoul, J. C. J., 91–128, 1982.

Cox, M. D. and Bryan, K.: A numerical model of the ventilated thermocline, J. Phys. Oceanogr., 14, 674–687, 1984.

Drago, A. F.: Development of a Capability in Physical Oceanography for the Maltese Islands, M. Phil. Upgrading Report, Dept. of Oceanography, University of Southampton, UK, 44–68, 1995.

Fox, A. D. and Maskell, A. J.: A nested primitive equation model of the Iceland Faeroe front, J. Geophysic. Res., 101, 18 259–18 278, 1996.

Galerpin, B. and Mellor, G. L.: A time-dependent, three-dimensional model of the Delaware Bay and river system, part 1, Description of the model and tidal analysis, Estuarine Coastal Shelf Sci., 31, 231–253, 1990.

Grancini, G. F.: Time Series of Ocean Data: Their use in offshore engineering. In: I.O.C. Technical Series: Time series of ocean measurements, 30, 17–22, 1985.

Grancini, G. F. and Michelato, A.: Current structure and variability in the Strait of Sicily and adjacent area, Ann. Geophysicae, 5, 75–88, 1987.

Hellerman, S. and Rosenstein, M.: Normal monthly wind stress over the world ocean with error estimates, J. Phys. Ocean., 13, 1093–1104, 1983.

Koch, S. E. and McQueen, J. T.: A survey of nested grid techniques and their potential for use within the MASS weather prediction model, NASA Technical Memorandum 87 808, 25, 1987.

Korres, G. and Lascaratos, A.: An eddy-resolving model of the Aegean and Levantine basins for the Mediterranean Forecasting System Pilot Project (MFSPP): implementation and climatological runs, Ann. Geophysicae, this issue, 2003.

Kostianoy, A. G., Astraldi, M., Gasparini, G. P., and Vignudelli, S.: Variability of the Sicilian Upwelling, In: IOC Workshop Report 159, Oceanic Fronts and Related Phenomena (Kostantin Federov Memorial Symposium), Pushkin, 279–283, 1998.

Legates, D. R. and Wilmott, C. J.: Mean seasonal and spatial variability in a gauge corrected global precipitation, Int. J. Climatology, 10, 121–127, 1990.

Lermusiaux, P. F. J.: Estimation and study of mesoscale variability in the Strait of Sicily, Dynamics of Atmosphere and Oceans, 29, 255–303, 1999.

Le Vourch, J., Millot, C., Castagne, N., Le Borgne, P., and Olry, J.-P.: Atlas of Thermal Fronts of the Mediterranean Sea derived from Satellite Imagery, Memoires de l'Institut oceanographique, Monaco, no. 16, VI-152 p., 1992.

MEDATLAS-I: A digital atlas of temperature and salinity of the Mediterranean Sea, Release on CD ROM by the MEDATLAS Consortium, 1997.

Manzella, G. M. R., Gasparini, G. P., and Astraldi, M.: Water exchange between the eastern and western Mediterranean through the Strait of Sicily, Deep-Sea Res., 35, 6, 1021–1035, 1988.

Mellor, G. L.: An equation of state for numerical models of oceans and estuaries, J. Atmos. Oceanic Tech., 8, 609–611, 1991.

Mellor, G. L. and Yamada, T.: Development of a turbulence closure model for geophysical fluid problems, Rev. Geophys. Space Phys., 20, 851–875, 1982.

Oey, L.-Y.: The formation and maintenance of density fronts on U.S. southeastern continental shelf during winter, J. Phys. Oceanogr. 16, 1121–1135, 1986.

Oey, L.-Y.: Eddy energetics in the Faroe-Shetland channel: a model resolution study, Con. Shelf Res., 17, 1929–1944, 1998.

Oey, L.-Y., and Chen, P.: A nested grid ocean model with application to the simulation of meanders and eddies in the Norwegian coastal current, J. Geophys. Res., 97, 20 063–20 086, 1992.

Oey, L.-Y. and Chen, P.: A model simulation of circulation in the northeast Atlantic shelves and seas, J. Geophys. Res., 97, 20 087–20 115, 1992.

Pinardi, N.: The Mediterranean Forecasting System Pilot Project, Scientific and Technical Plan, Package II, 92, 1998.

Pinardi, N. and Masetti, E.: Variability of the large-scale general circulation of the Mediterranean Sea from observations and modelling: a review, Palaeo-3, 15 May 2000, 158, 153–173, 2000.

Pinardi, N., Auclair, F., Cesarini, C., Demirov, E., Umani, S. F., Giani, M., Montanari, G., Oddo, P., Tonani, M., and Zavatarelli, M.: Toward marine environmental predictions in the Mediterranean Sea coastal areas: Monitoring approach, in: Ocean Forecasting: Conceptual Basis and Applications, (Eds) Pinardi, N.

and Woods, J. D., Springer, 339–376, 2002.

Pinardi, N., Korres, G., Lascaratos, A., Roussenov, V., and Stanev, E.: Numerical simulation of the interannual variability of the Mediterranean Sea upperocean circulation, Geophys. Res. Lett., 24, 425–428, 1997.

Pinardi, N., Antoine, D., Babin, M., Baretta, J., Bassini, S., Brenner, S., Crepon, M., Cruzado, A., Dandin, P., De May, P., Drago, A. F., Evensen, G., Gacic, M., Gasparini, G. P., Hamza, W., Lascaratos, A., Le Traon, P.-Y., Garcia, Lopez, M. A., Maillard, C., Manzella, G. M. R., Millot, C., Raicich, F., Raillard, O., Reid, P. C., Sorgente, R., Thanos, I., Triantafyllou, G., Tziavos, C., and Zodiatis, G.: The Mediterranean ocean forecasting system: the first phase of implementation, Proceedings published in OCEANOBS 99 Conference, 1999.

Robinson, A. R., Arango, H. G., Varnas, A. W., Leslie, W. G., Miller, A. J., Haley, P. J., and Lozano, C. J.: Real-time regional forecasting in modern approaches to data assimilation in ocean modelling, in: Modern approaches to data assimilation in ocean modelling, (Ed) Melanotte-Rizzoli, P., Elsevier Science B.V., 377–410, 1996.

Sorgente, R., Drago, A. F., and Ribotti, A.: Seasonal variability in the Central Mediterranean Sea Circulation, Ann. Geophysicae, this issue, 2003.

Spall, M. A. and Holland, W. R.: A nested primitive equation model for oceanic applications, J. Phys. Oceanogr., 21, 205–220, 1991.

Warn-Varnas, A., Sellschops, J., Haley, P. J. Jr., Leslie, W. G., and Lozano, C. J.: Strait of Sicily water masses, Dynamics of Atmosphere and Oceans, 29, 437–469, 1999.

Wolanski, E.: Biology and physics links, in: Changing Estuaries and Coastal Environments, (Eds) Salomons, W., Bayne, B., Heap, C., and Turner, K., GKSS Research Centre, Geessthacht, Germany, 268 pp., 1995.

Wust, G.: On the vertical circulation of the Mediterranean Sea, J. Geoph. Res., 66, 3261–3271, 1961.

Zavatarelli, M., Pinardi, N., Kourafalou, V. H., and Maggiore, A.: Diagnostic and prognostic model studies of the Adriatic Sea general circulation: Seasonal variability, J. Geophys. Res., 107–120, 2002.